Deciphering the enzymatic mechanisms of short-chain dehydrogenase/reductase epimerases and decarboxylases

Debanić, Fran

Master's thesis / Diplomski rad

2021

Degree Grantor / Ustanova koja je dodijelila akademski / stručni stupanj: **University of Zagreb, Faculty of Food Technology and Biotechnology / Sveučilište u Zagrebu, Prehrambeno-biotehnološki fakultet**

Permanent link / Trajna poveznica: https://urn.nsk.hr/urn:nbn:hr:159:077009

UNIVERSITY OF ZAGREB
FACULTY OF FOOD TEHCNOLOGY AND BIOTECHNOLOGY

GRADUATE THESIS

Zagreb, July 2021.

Fran Debanić
1277/BPI

SVEUČILIŠTE U ZAGREBU
PREHRAMBENO-BIOTEHNOLOŠKI FAKULTET

DIPLOMSKI RAD

Zagreb, srpanj 2021.

Fran Debanić
1277/BPI

DECIPHERING THE ENZYMATIC MECHANISMS OF SHORT-CHAIN DEHYDROGENASES/ REDUCTASES EPIMERASES AND DECARBOXYLASES

Experimental work of this Graduate Thesis was done at the Institute of Biotechnology and Biochemical Engineering at Graz University of Technology. The Thesis was made under the guidance of prof. dr. sc. Bernd Nidetzky and with the help of Annika Jasmin Eveliina Borg, PhD. Thesis was done at Faculty of Food Technology and Biotechnology at University of Zagreb under the guidance of prof. dr. sc. Anita Slavica, Faculty of Food Technology and Biotechnology University of Zagreb.

BASIC DOCUMENTATION CARD

Graduate Thesis

University of Zagreb
Faculty of Food Technology and Biotechnology
Department of Biochemical Engineering
Laboratory of Biochemical Engineering, Industrial Microbiology and Malting and Brewing Technology

Scientific area: Biotechnical Sciences
Scientific field: Biotechnology

DECIPHERING THE ENZYMATIC MECHANISMS OF SHORT-CHAIN DEHYDROGENASE/REDUCTASE EPIMERASES AND DECARBOXYLASES

Fran Debanić, 1277/BPI

Abstract: UDP-GlcA methyl ester, a substrate analogue for short-chain dehydrogenase/reductase epimerases and decarboxylases - human UDP-Xylose synthase (UXS), UDP-Apiose/Xylose synthase (UAXS) and UDP-glucuronic acid 4-epimerase (UGAepi), was successfully synthesized and purified, and thus enabled investigation of their enzymatic mechanisms. The three enzymes were expressed in *E. coli* and purified to homogeneity. Both decarboxylases (UXS and UAXS) converted UDP-GlcA methyl ester (0.71 U/mg and 0.03 U/mg, respectively) in a comparable manner to conversion of their natural substrate - UDP-glucuronic acid (UDP-GlcA, 1.6 U/mg and 0.15 U/mg, respectively). Newly established methanol assay proved that the two decarboxylases hydrolyze the ester before the decaborxylation reaction while UGAepi does not perform the hydrolysis. UGAepi epimerizes faster the substrate analogue (0.65 U/mg) than the natural substrate (0.53 U/mg). Additionaly, gene encoding UAXS from *Geminococcus roseus* was successfully expressed in *E. coli* and resulting enzyme (GrUAXS) posses' lower activity towards UDP-GlcA (2.1 mU/mg) than its mutant (S120C; 12.3 mU/mg) supporting the importance of cysteine residue in the active site of the enzyme.

Keywords: GrUAXS, UAXS, UDP-glucuronic acid methyl ester, UGAepi, UXS

Thesis contains: 69 pages, 36 figures, 17 tables, 21 references, 00 supplements

Original in: English

Graduate Thesis in printed and electronic (pdf format**) version is deposited in:** Library of the Faculty of Food Technology and Biotechnology, Kačićeva 23, Zagreb.

Mentor: *Univ.-Prof. Dipl.-Ing. Dr.techn. Bernd Nidetzky, prof.dr.sc. Anita Slavica*

Technical support and assistance: *Annika Jasmin Eveliina Borg, PhD*

Reviewers:
1. *Mirela Ivančić Šantek,* Full professor
2. *Anita Slavica,* Full professor
3. *Blaženka Kos,* Full professor
4. *Renata Teparić,* Full professor (substitute)

Thesis defended: July 23rd, 2021

TEMELJNA DOKUMENTACIJSKA KARTICA

Diplomski rad

Sveučilište u Zagrebu
Prehrambeno-biotehnološki fakultet
Zavod za biokemijsko inženjerstvo
Laboratorij za biokemijsko inženjerstvo,
industrijsku mikrobiologiju i tehnologiju piva i slada

Znanstveno područje: Biotehničke znanosti
Znanstveno polje: Biotehnologija

ISTRAŽIVANJE REAKCIJSKIH MEHANIZAMA KRATKOLANČANIH DEHIDROGENAZA/REDUKTAZA EPIMERAZA I DEKARBOKSILAZA

Fran Debanić, 1277/BPI

Sažetak: UDP-GlcA metil ester, analog supstrata za kratkolančane dehidrogenaze/redukataze epimeraze i dekarboksilaze - humanu UDP-ksiloza sintazu (UXS), UDP-apioza/ksiloza sintazu (UAXS) i UDP-glukuronska kiselina 4-epimerazu (UGAepi), uspješno je sintetiziran i pročišćen, čime je omogućeno istraživanje enzimskih mehanizama ovih katalizatora. Tri enzima su eksprimirana u stanicama *E. coli* i pročišćena. Obje dekarboksilaze (UXS and UAXS) su konvertirale UDP-GlcA metil ester (redom 0.71 U/mg i 0.03 U/mg) slično konverziji njihova prirodnog supstrata - UDP- glukuronske kiseline (UDP-GlcA, redom 1.6 U/mg i 0.15 U/mg). Pomoću novoustanovljene metode za određivanje metanola utvrđeno je da dvije dekarboksilaze hidroliziraju ester prije reakcije dekarboksilacije, dok UGAepi ne provodi hidrolizu estera. UGAepi brže epimerizira analog supstrata (0.65 U/mg) nego svoj prirodni supstrat (0.53 U/mg). Dodatno, gen koji kodira UAXS iz *Geminococcus roseus* je uspješno eksprimiran u *E. coli* i dobiveni enzim (GrUAXS) ima nižu aktivnost prema UDP-GlcA (2.1 mU/mg) nego njegov mutant (S120C, 12.3 mU/mg), što podupire važnu ulogu cisteina u aktivnom mjestu ovoga enzima.

Ključne riječi: GrUAXS, UAXS, UDP-glukuronksa kiselina metil ester, UGAepi, UXS

Rad sadrži: 69 stranica, 36 slika, 17 tablica, 21 literaturnih navoda, 00 priloga

Jezik izvornika: engleski

Rad je u tiskanom i elektroničkom (pdf format) obliku pohranjen u: Knjižnica Prehrambeno-biotehnološkog fakulteta, Kačićeva 23, Zagreb

Mentor: *Univ.-Prof. Dipl.-Ing. Dr.techn. Bernd Nidetzky, prof.dr.sc. Anita Slavica*

Pomoć pri izradi: *Annika Jasmin Eveliina Borg, PhD*

Stručno povjerenstvo za ocjenu i obranu:
1. Prof.dr.sc. *Mirela Ivančić Šantek*
2. Prof.dr.sc. *Anita Slavica*
3. Prof.dr.sc. *Blaženka Kos*
4. Prof.dr.sc. *Renata Teparić* (zamjena)

Datum obrane: 23. srpnja 2021.

Table of contents

1. INTRODUCTION

The short-chain dehydrogenase/reductase (SDR) enzyme superfamily has raised much interest lately, mainly because of the capability to catalyze various different reactions regardless the SDRs structural similarities. This work focuses on human UDP-Xylose synthase (UXS), UDP-Apiose/Xylose synthase (UAXS) from *Arabidopsis thaliana* and UDP-glucuronic acid 4-epimerase (UGAepi) from *Bacillus cereus*. UXS and UAXS are members of the SDR-type decarboxylases and have a lot of structural characteristics in common. Despite their similarities, these enzymes follow completely different reaction mechanisms with the same substrate (UDP-glucuronic acid), except the first step of the reaction which they share. UAXS is able to carry out an extremely complex reaction, a fascinating for a single enzyme. Its mechanism considers oxidations and reductions through NADH/NAD^+ coupling, challenging rearrangements of sugar ring and aldol/retro-aldol reactions. It is believed that UAXS can choose between the UXS pathway and produce UDP-Xylose, and, as the second option - so called its own pathway and produce UDP-Xylose and UDP-Apiose.

On the other side, UGAepi catalyzes the epimerization UDP-glucuronic acid to UDP-galacturonic acid and also shares the first step of the reaction with UXS and UAXS. Unlike UXS and UAXS, UGAepi is able to prevent the decarboxylation of the substrate.

The aim of this work is to synthesize the substrate analogue UDP-glucuronic acid methyl ester which is then used for testing activity of these enzymes in order to better understand the importance of certain amino acid residues in their active sites which are responsible for decarboxylation (UXS and UAXS) or epimerization (UGAepi). The synthesis route of UDP-glucuronic acid methyl ester is planned to be accomplished in two enzymatic steps. The first step is phosphorylation of glucuronic acid methyl ester by glucuronic acid kinase and forming glucuronic acid methyl ester 1-phosphate. The second step is the nucleotidyl transfer reaction of glucuronic acid methyl ester 1-phosphate by UDP-glucose pyrophosphorylase to produce UDP-glucuronic acid methyl ester. Further steps in the substrate preparation include isolation and purification of UDP-glucuronic acid methyl ester by using improved ethanol precipitation protocol. The purified UDP-glucuronic acid methyl ester is then used as a substrate for UXS, UAXS and UGAepi.

Alongside plant UAXS, this enzyme has been recently discovered in bacteria. This thesis puts focus on the variant from *Geminococcus roseus* (GrUAXS) which has one very big structural difference compared to plant UAXS. GrUAXS has serine (Ser120) instead of cysteine (Cys140) in plant UAXS. This work is aiming to mechanistically characterize GrUAXS by expressing it in *E. coli* BL21 (DE3) LEMO21 expression strain and then test activity of expressed

heterologous protein with UDP-glucuronic acid. The experiments also include introducing the mutation in GrUAXS on a position 120 by replacing serine with cysteine.

2. THEORETICAL PART

2.1 SDR SUPERFAMILY

The short-chain dehydrogenases/reductases (SDRs) are a part of the large enzyme family of NAD(P)(H)-dependent oxidoreductases and share common sequence motifs and mechanistic characteristics (Kavanagh et al., 2008). These enzymes are involved in many different metabolisms of: amino acid, carbohydrate, lipid, cofactor, hormon and xenobiotic as well as redox sensor mechanisms (Kavanagh et al., 2008).

According to the current classification based on protein chain lenght, mechanistic and structural properties, dehydrogenases/reductases are separated into three groups: short, medium and long chain (Jörnvall et al., 1995; Oppermann et al., 2003). The common motif that occurs in all groups of SDRs is the Rossman-fold composed of β-sheet constructed of 6-7 β-strands with 3-4 α-helices flanked on each side (Kavanagh et al., 2008). Unlike medium-chain dehydrogenases/reductases (MDRs) and long-chain dehydrogenases/reductases (LDRs), most of the SDRs have only one substrate binding catalytic site located in the C-terminal region (Kavanagh et al., 2008).

The SDR superfamily contains about 1/4 of all known dehydrogenases (Kallberg and Persson, 2006) and consists of at least 47000 characterized enzymes (Kallberg et al., 2010). SDRs can be found in all domains of life, mostly in bacteria considering that a large number of completely sequenced genomes have a bacterial origin (Kavanagh et al., 2008). In Figure 1, the examples of common reactions catalyzed by SDRs are shown.

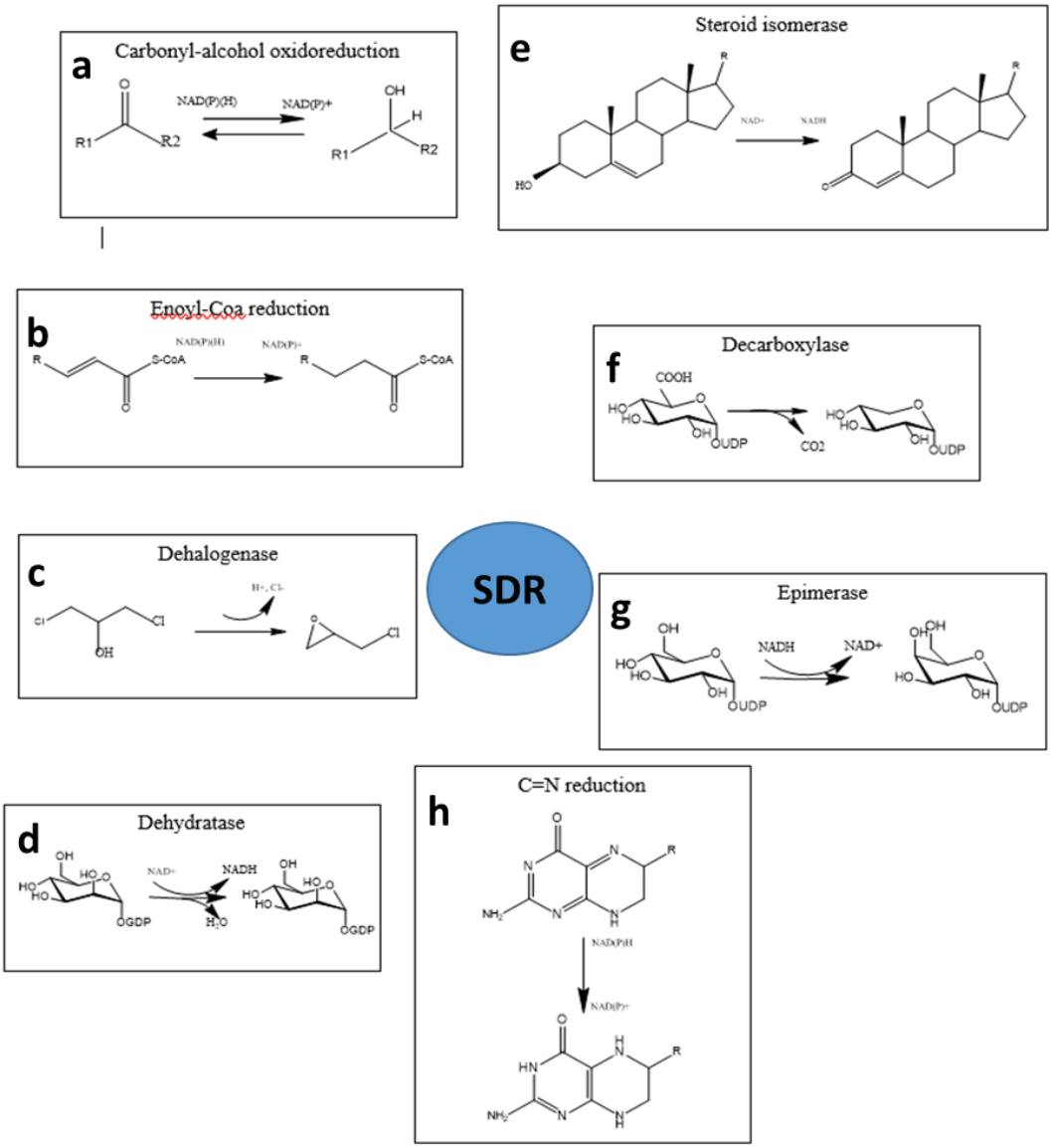

Figure 1. Examples of reactions catalyzed by SDRs: (a) Carbonyl-alcohol oxidoreduction, (b) Enoyil-Coa reduction, (c) Dehalogenation, (d) Dehydration of GDP-mannose to GDP-4-keto-6-deoxy-mannose by GDP-4-keto-6-deoxy-mannose dehydratase, (e) Steroid isomerase, (f) Decarboxylation of UDP-glucuronic acid to UDP-Xyl by UDP-xylose synthase, (g) Epimerization of UDP-Glc to UDP-Gal by UDP-glucose 4-epimerase, (h) C=N reduction Reproduced and modified from Kavanagh et al. (2008).

Based on the chain lenght, two main types of SDRs exist - classical (chain lenght of about 250 amino acid residues) and extended (chain lenght of about 350 amino acid residues) (Kavanagh et al., 2008). There are also three futher SDR subfamilies; intermediate, complex and divergent, distinguished by the cofactor binding sequence motifs (Kavanagh et al., 2008).

The Rossman-fold scaffold binding NAD(P)(H), shared among all the members of the SDR superfamily, is the only merging criterion following the sequencing of enzymes (Kavanagh et al., 2008). The majority of SDRs display a Tyr-based catalytic center and the reaction often proceeds through an ordered „bi-bi“ mechanism, which means that the cofactor binds first and leaves last (Kavanagh et al., 2008).

In a comparison with classical SDRs, extended SDRs use the basic SDR catalytic machinery [as well as tightly bound NAD(P)(H)] which is a highly conserved Asn/Ser/Tyr/Lys tetrad, and are able to perform a wide spectrum of reactions, *e.g.* epimerization, decarboxylation and ring opening initiated by aldol cleavage (Borg et al., 2021b).

Regarding the oligomeric state, most of the SDRs have homodimeric or homotetrameric structures (Kavanagh et al., 2008).

The main extended SDR groups are: SDR-type epimerases, SDR-type dehydratases, SDR-type isomerases and SDR-type decarboxylases (Borg et al., 2021a; Kavanagh et al., 2008). The enzymes studied in this thesis - UDP-Xylose synthase (UXS), UDP-Apiose/xylose synthase (UAXS) and UDP-glucuronic acid 4-epimerase (UGAepi), belong to the extended SDRs subfamily, specifically into the groups of SDR decarboxylases (UXS and UAXS) and SDR epimerases (UGAepi) (Borg et al., 2021a; Kavanagh et al., 2008). Besides the enzyme classes mentioned above, the SDRs superfamily is formed by addition of SDR lyases(Kavanagh et al., 2008). The initial step characterizing all of these types of SDRs is the oxidoreduction of the certain substrate (Kavanagh et al., 2008). To prove this fact, the NAD(P)(H) cofactor is always bound to these enzymes (Kavanagh et al., 2008).

UGAepi, one of the main focuses of this thesis, has been characterized recently (Borg et al., 2021b). UXS and UAXS are part of SDR-type decarboxylases (Borg et al., 2021a) and share some of the mechanistic properties with the epimerases (Kavanagh et al., 2008). UAXS and UXS perform a similar reaction mechanism (as shown in Figure 2) in terms of the initial reaction step, with the major difference that UAXS is able to perform the sugar ring contraction and produce UDP-Apiose (Borg et al., 2021a; Eixelsberger et al., 2012; Savino et al., 2019).

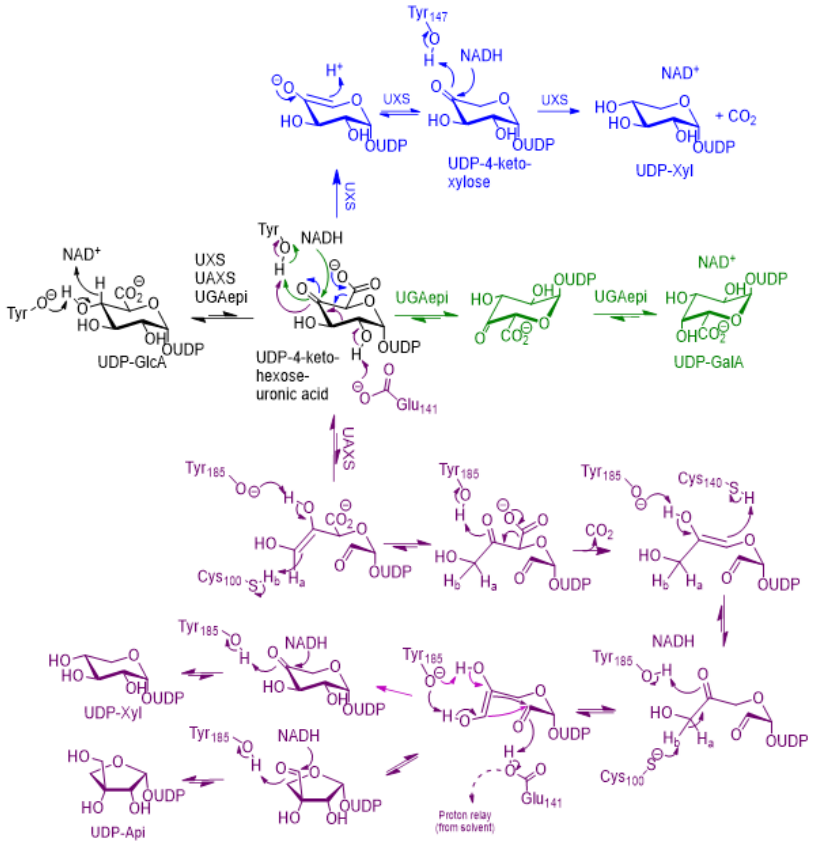

Figure 2. The proposed reaction mechanisms of UXS (blue), UAXS (purple) and UGAepi (green). All of the three enzymes share the first oxidoreduction step of UDP-GlcA (black). After UDP-4-keto-hexose-uronic acid is formed, their pathways separate. Reproduced and modified from Borg et al. (2021a).

The interest for the enzymes from SDR superfamily has risen recently, since their applications in biotechnological and pharmaceutical purposes have a huge potential. These enzymes are also known as a „druggable“ enzyme class considering their perpective in a drug production (Kavanagh et al., 2008).

2.2 NUCLEOSIDE-DIPHOSPHATE (NDP) – SUGAR INTERCONVERSION ENZYMES: UXS, UAXS and UGAepi

Enzymes involved in the conversion of nucleotide-diphospho-sugars (NDP-sugars) are often named as NDP-sugar interconversion enzymes (NSEs) existing in all domains of life (Yin et al., 2011). In plants, there are more than 30 different NDP-sugars and they mostly play a role

in the synthesis of various cell wall polysaccharides, but also have a potential in a biofuel production (Yin et al., 2011).

Observing that many of these plant enzymes catalyze a series of reactions converting similair types of NDP-sugars, the origin of those enzymes is still not well known (Yin et al., 2011). The study carried out by Yin et al. (2011) shows that the plant NSEs families diverged anciently.

The enzymes (UXS, UAXS, UGAepi), which are the main interest of this thesis, have the common ancestor dating far in the past, from the ancient prokaryotic world. The ancestor of NADP_Rossmann clan contained the *Epimerase* domain (conserved GxxGxxG motif) which is responsible for binding ATP/NAD/NADP in N-terminal region (Yin et al., 2011). Moreover, it is obvious that UAXS, UXS and UGAepi diverged from the last common ancestor Epimerase Superfamily A into two enzyme classes - decarboxylases and 3,5-epimerases (Yin et al., 2011).

UXS, UAXS and UGAepi convert the same substrate, UDP-glucuronic acid (UDP-GlcA), by the same intial reaction step (Figure 2) which is oxidation of the substrate at the C4 (Borg et al., 2021b). The UDP-GlcA has the central role in the synthesis of other NDP-sugars either being decarboxylated to UDP-Apiose (UDP-Api) or UDP-Xylose (UDP-Xyl) (Eixelsberger et al., 2012; Savino et al., 2019) or epimerized to UDP-galactouronic acid (UDP-GalA) by UGAepi through Leloir pathway (Allard et al., 2001; Borg et al., 2021b). Furthermore, UDP-Xyl serves as an important sugar donor for the synthesis of glycoproteins, polysaccharides, oligosacharides and can be found in animals, plants, fungi and bacteria (Harper and Bar-Peled, 2002). On the other hand, UDP-Api was believed to be present only in plants, but it has been found in bacteria recently. Therefore, it is still unknown why some bacterial species developed the ability to synthesize the apiosides (Smith and Bar-Peled, 2017). In plants, the polysaccharides containing apiose are an important part of the cell wall pectic polymers as well as the apiosylated secondary metabolites (Smith and Bar-Peled, 2017). Although the phylogenetic analysis reveals distinguishing origins between bacterial and plant UAXSs, there was no difference in products formed; both enzymes produce UDP-Api and UDP-Xyl.

UGAepi was studied in *E. coli*, humans (Allard et al., 2001) and most recently the variant from *Bacillus cereus* (Borg et al., 2021b). *E. coli*-type epimerase share 55% of structure with the human-type and both are homodimeric (Allard et al., 2001). In humans, the UGAepi deficiency is characterized in only red and white blood cells or the other tissues (Allard et al., 2001).

The substrate analogues resemble a powerful tool for getting insight into mechanistics of UXS, UAXS and UGAepi. Regarding that, the focus in this thesis is on UDP-GlcA methyl ester, the analogue of UDP-GlcA which these enzymes naturally transform to the either UDP-Xyl and UDP-Api or in the case of epimerase, to UDP-GalA (Borg et al., 2021b; Savino et al., 2019).

The methyl group instead of C6 hydroxyl group of substrate could gives the possibility to (1) find out whether UXS and UAXS are able to perform the hydrolysis of the ester bond and perform the decarboxylation, and (2) what is the mechanism behind that. UDP-GlcA methyl ester enables studying the importance of the amino-acid residues involved in preventing the decarboxylation and ensuring the epimerization of the substrate. UGAepi has Arg185 residue in its active site which is responsible for binding the carboxylate of UDP-GalA (Borg et al., 2021b). UDP-GlcA methyl ester does not have a negatively charged carboxylate, but it has the neutral methyl ester moiety. Therefore, UDP-GalA cannot be bound by UGAepi Arg185 which gives the possibility to define the amino acid residues important for preventing the decarboxylation.

2.2.1 UAXS and UXS decarboxylation mechanisms

As mentioned previously, both UXS and UAXS enzymes catalyze the conversion of UDP-GlcA to UDP-Xyl. In addition, UAXS performs a complex, challenging reaction and is able to form UDP-Api alongside UDP-Xyl. On contrary, UXS displays the fast decarboxylation of UDP-GlcA by performing the ring distortion to have the carboxylate in an axial position and produce only UDP-Xyl (Borg et al., 2021a). The UXS activity has been observed in mammals, plants and bacteria with about 57% sequence identity shared between human (hUXS) and various bacterial enzyme forms (Eixelsberger et al., 2012). However, hUXS represents one of the best characterized form among all existing UXSs and shows relation with other SDRs; a substrate binding domain and an NAD^+ binding domain (Eixelsberger et al., 2012). The reaction starts by oxidation of the C4 hydoxyl group in UDP-GlcA by tyrosine in the active site and enzyme-bound NAD^+ and this first reaction is followed by decarboxylation of UDP-4-keto-hexose-uronic acid formed in the first step(Eixelsberger et al., 2012) and resembles a typical SDR mechanism common with other enzymes belonging to that family(Borg et al., 2021a). This mechanism is shown in Figure 3.

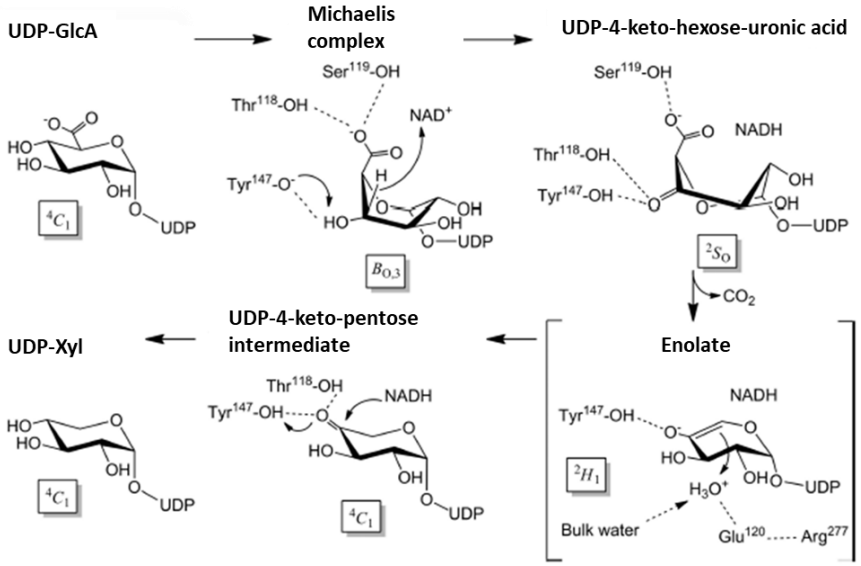

Figure 3. The reaction mechanism of hUXS. Tyr147, as the catalytic base, initiates the oxidation of C4 hydroxyl group in UDP-GlcA .Reproduced and modified from Eixelsberger et al. (2012).

The active site of hUXS has a classical SDR type catalytic center containing Thr118, Tyr147 and Lys151 with addition of Ser119, Glu120 and Arg277, which is specific for UXS group of enzymes (Eixelsberger et al., 2012).

The conversion of UDP-GlcA to UDP-Xyl is a three-step reaction including a pyranose ring distortion (Figure 4; (Eixelsberger et al., 2012). In order to establish a proper conformation to start the reaction, Glu120 and Arg277 interact and fasten together two long loops of the enzyme and close the active site. This leads to bringing the Thr118 and Ser119 into their reactive positions. Additionally, these two residues (Thr118 and Ser119) form hydrogen bonds with the substrate at the carboxylate group at C5 (Eixelsberger et al., 2012). Tyr147 is responsible for oxidizing the substrate at C4 forming UDP-4-keto-hexose uronic acid, the reaction intermediate (Eixelsberger et al., 2012). Thr118 keeps the substrate in a correct orientation while the decarboxylation occurs at C5 and Tyr147 stabilizes the enolate (Eixelsberger et al., 2012). Glu120 and Arg277 coordinate a molecule of water and support the protonation of C5 yielding UDP-4-keto-pentose trapped in the enzyme's active site (Eixelsberger et al., 2012). The final step, reduction of the keto-group using NADH with help of Tyr147 forms UDP-Xyl (Eixelsberger et al., 2012). In the case of UAXS, the sugar ring opening is the key step for UDP-Xyl biosynthesis while UXS causes the ring distortion without opening it (Borg et al., 2021a; Eixelsberger et al., 2012; Savino et al., 2019).

On the other hand, UAXS shares the initial reaction step with UXS, but proceeds to form UDP-Xyl following a fundamentally different mechanism (Borg et al., 2021b). UAXS also produces a pentose sugar UDP-Apiose (Smith and Bar-Peled, 2017). Eixelsberger et al. (2017) conducted a study to prove the ring-opening mechanism during the UDP-Api/UDP-Xyl synthesis by using the UDP-2-deoxy glucuronic acid as a substrate analogue. In contrast to UXS, UAXS has a Cys100 and Cys140 residues in its active site making it a distinct feature compared to typical SDRs (Savino et al., 2019). It is still a mystery why UAXS and UXS, considering their structural similarity, are able to produce different products through different pathways utilizing the same subtrate UDP-GlcA. The answer is most likely in a stereo-electronic control of reaction selectivity and the Cys100 and Cys140 (Borg et al., 2021a). Given that the ring-opening occurs before the decarboxylation, it is neccesary to consider stereo-electronic conditions favoring the decarboxylation. In general, as shown in Figure 4, the decarboxylation is favored when the dihedral angle between C=O bond and the cleaved C-C bond is approximately 90° (Borg et al., 2021a), meaning an axial carboxylate moiety.

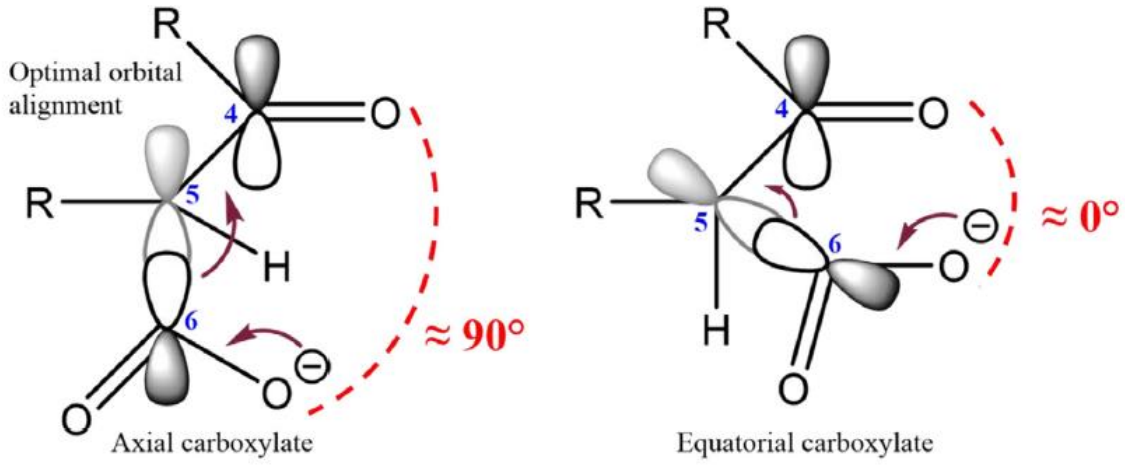

Figure 4. Orbital alignment in decarboxylation of a β-keto acid with the axial (left) and equatorial (right) carboxylate moiety (reproduced from Borg et al., 2021a).

The idea of stereo-electronic control has been proven on UXS mechanism by studying the Michaelis complex formed by binding the substrate NAD^+ (Borg et al., 2021a). Molecular dynamics computational studies have shown that $^4C_1$ pyranose chair had to be distorted in $B_{o,3}$ boat confirmation in order to place the carboxylate in an axial position (Eixelsberger et al., 2012). Interestingly, UAXS seems to be able to control the timing of decarboxylation. The

decarboxylation at C5 can occur only when the ring has opened and the carboxylate is brought to axial position (Borg et al., 2021a; Savino et al., 2019).

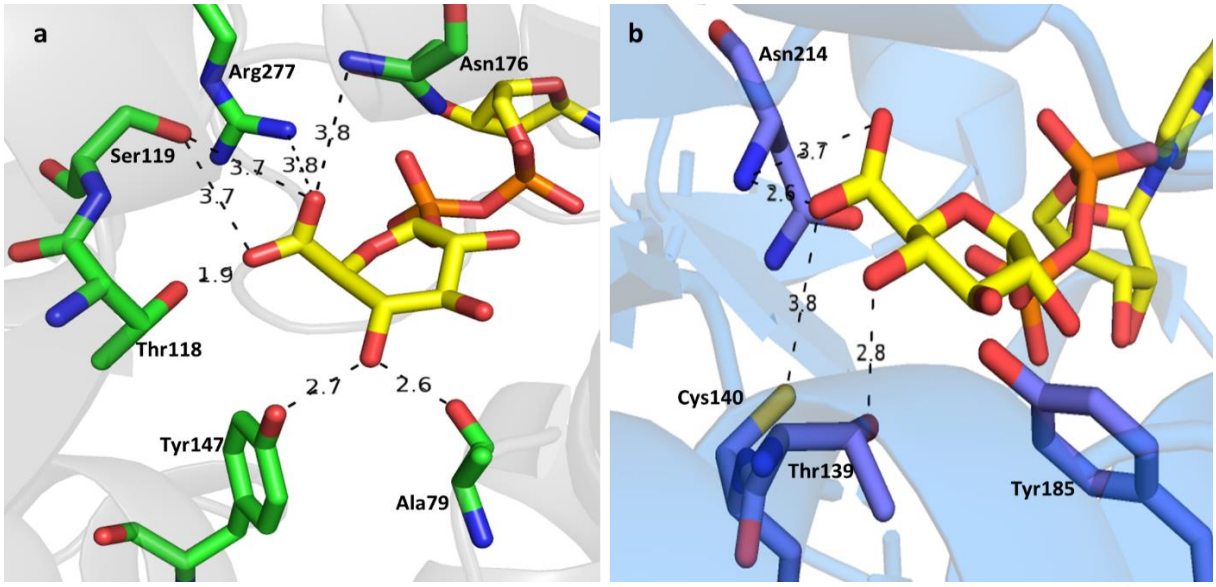

Figure 5. Active site close-ups of UXS (a) and UAXS (b) showing the interactions between amino-acid residues and carboxylate moiety of UDP-GlcA. The interactions with hydroxyl group at C4 are shown additionally (a) The substrate complex of UXS (grey; PDB: 2B69; https://www.rcsb.org/structure/2B69, accessed on July 8th 2021) with UDP-GlcA shows the carboxylate in an axial position (b) The substrate complex of UAXS (blue; PDB: 6H0P; https://www.rcsb.org/structure/6H0P, accessed on July 8th 2021) with UDP-GlcA shows the carboxylate in an equatorial position (Borg et al., 2021a).

The study with the UAXS C100S variant, by following deuterium incorporation at C3, revealed the importance of Cys100 in the ring opening step and the enzyme was not able to synthesize any UDP-Api (Savino et al., 2019). The isotope labelling suggests that UXS ring distortion route was used (Savino et al., 2019) and it is not suprising since those two enzymes (UXS and UAXS) belong to the same family, and share many structural features (Kavanagh et al., 2008). Furthermore, the active site of UAXS is unusually flexible enabling the enzyme to keep the carboxylate initially in an equatorial position disfavoring the fast decarboxylation (Borg et al., 2021a). The pyranosyl ring of UDP-GlcA can adopt multiple conformations that deviate from $^4C_1$ chair conformation while still being able to have a proper positioning for hydride transfer to the NAD^+. Glu141 and Tyr105 are involved in the ring-opening by forming hydrogen bonds with the hydroxyl group at C2. Glu141 is the base which deprotonates the hydroxly group at

C2 in the end of that step of the reaction. Cys140 supports the decarboxylation step by protonating C5 and Cys100 has the flexibility of its side chain regarding the fact that the side chain is pointing out of and into the active site (Savino et al., 2019). Cys100 is also responsible for the proton transfer to C3 (Savino et al., 2019).

2.2.2 UGAepi rotation mechanism

UGAepi as a member of SDR-type epimerases is evolutionary related to the SDR decarboxylases UXS and UAXS (Borg et al., 2021b). The mutagenesis study with Y149F variant showed the evidence that Tyr149 is the residue responsible for catalytic activity for oxidation (Borg et al., 2021b). The hydride transfer from C4 to the enzyme-bound NAD^+ with Tyr as a catalytic base to form the UDP-4-keto-hexose-uronic acid intermediate is the first step of the reaction – after that, the pathways of UXS, UAXS and UGAepi separate (Borg et al., 2021b). The specialty of UGAepi is its ability to keep the carboxylate in an equatorial position avoiding decarboxylation and forming UDP-GalA from UDP-GlcA (Borg et al., 2021b). Therefore, UGAepi is able to perform the 180° rotation of the formed keto-intermediate (Borg et al., 2021b).

Considering that the β keto intermediate produced after the initial oxidation step is very labile and prone to decarboxylation, it is interesting that UGAepi has the ability to prevent decarboxylation. Figure 6 shows the carboxylate binding interactions and the SDR catalytic dyad. The carboxylate of the substrate is trapped in hydrogen bond network of four residues: Thr126, Ser127, Ser128 and Thr178 (Borg et al., 2021b). The 4-keto intermediate is prone to decarboxylation, therefore UGAepi faces the task to prevent the decarboxylation in order to enable a free rotation of sugar moeity and produce UDP-GalA (Borg et al., 2021b). Additionally, UGAepi lacks the Cys140 residue involved in a proton transfer to C5 during the decarboxylation of the intermediate, in contrast to UXS and UAXS (Borg et al., 2021b). To provide the epimerization, UGAepi has a slighlty different binding pocket with Ser128 instead of Glu in UXS/UAXS. The other major difference is that the Thr126 from the SDR catalytic triad is in a hydrogen bond distance from C5 carboxylate and 4-OH of the substrate (Borg et al., 2021b). NAD^+ and the substrate are bound in their binding sites deep and tightly, disabling the possibility of changing the carboxylate moeity to axial, which would lead to decarboxylation of the intermediate (Borg et al., 2021b).

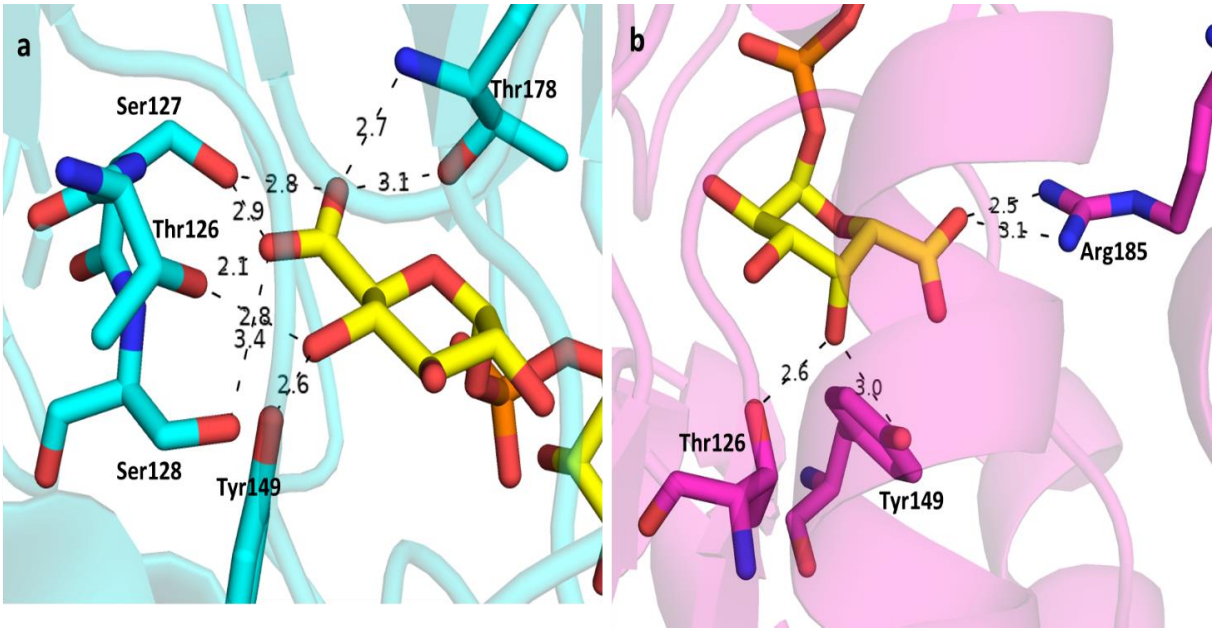

Figure 6. The active site close-ups of UGAepi from *Bacillus cere*us (BcUGAepi) in complexes with UDP-GlcA (a, light blue; PDB: 6ZLD; https://www.rcsb.org/structure/6ZLD, accessed on July 8th 2021) and UDP-GalA (b, purple; PDB: 6ZLL; https://www.rcsb.org/structure/6ZLL, accessed on July 8th 2021). In both cases, the carboxylate moiety is equatorial. Arg185 residue stabilizies the carboxylate of UDP-GalA and prevents the decarboxlyation (Borg et al., 2021a).

2.3 A NOVEL UDP-APIOSE/XYLOSE SYNTHASE GrUAXS FROM MARINE PHOTOTROPH *Geminococcus roseus*

Smith and Bar-Peled (Smith and Bar-Peled, 2017) published a discovery of apiosyl residue during the screening for nover bacterial glycans in the methanolic extracts of the *Geminococcus roseus* and *Xanthomonas pisi.* Prior to that, it was assumed that apiosides are present only in plants (Smith and Bar-Peled, 2017). Besides UXS, UAXS and UGAepi, the UDP-Apiose/UDP-Xylose synthase from *Geminococcus roseus* (GrUAXS) was also studied in this thesis.

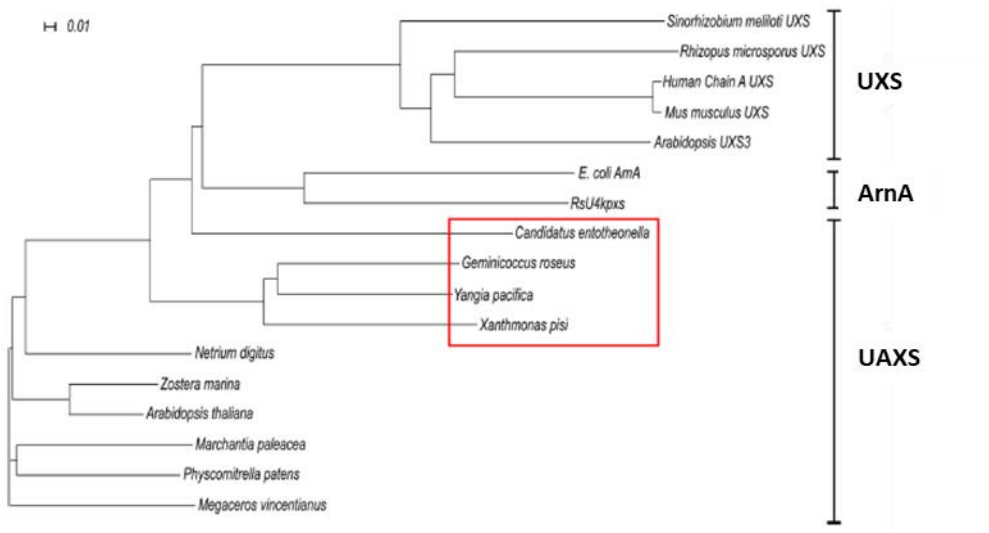

Figure 7. The phylogenetic tree of the enzymes involved in the synthesis of UDP-Apiose. UAXSs, which have the bacterial origin, are shown in red square(Smith and Bar-Peled, 2017)

Figure 7 shows that bacterial UAXSs (bUAXS) are phylogenetically distinct from other SDRs sharing a branch with the plant UAXSs. The species containing these enzymes were isolated from various sources, for instance soil and sea (Smith and Bar-Peled, 2017). According to the current genomic database, only eight bUAXSs exist with potentially increasing number in future considering that more marine bacteria are going to be sequenced (Smith and Bar-Peled, 2017). Based on the sequence identity, there is a possibility that every bUAXS has a distinct ancestor (Smith and Bar-Peled, 2017). Regardless of the origin of bUAXSs, they have the same domains and catalytic activity as plant UAXSs (Smith and Bar-Peled, 2017). Interestingly, the genes coding for bUAXSs are found in a bacteria isolated from various soruces - *e.g.* sea and soil, supporting the fact that bacteria require that enzyme specifically for the UDP-Apiose synthesis (Smith and Bar-Peled, 2017). Most likely, the apiose is being incorporated as a secondary metabolite or cell wall glycan representing that feature as an advantage for the enviroment where these species live (Smith and Bar-Peled, 2017). Further studies on bUAXSs could lead to the discovery of the potential new biosynthesis pathways. GrUAXS is interesting for this thesis since it has Ser instead of Cys140 found in plant UAXS (*Arabidopsis thaliana*). Cys140 actively participates in sugar ring closing and protonating the C5 of the intermediate after decarboxylation, as well as in a rearrangement of the ring opened structure (Savino et al., 2019). Changing Cys(140) to Ser might lead to either unability of forming the UDP-Xyl and UDP-Api or a signifcantly lower activity, as proven by Savino et al. (2019) by working with C140S variant of plant UAXS from *Arabidopsis thaliana*.

3. EXPERIMENTAL PART

3.1 MATERIALS

Table 1 shows all the chemicals and compounds used during the experimental work. Table 2 contains all media. E. coli strains used for transformation and expression are shown in Table 3. Plasmid used for transformation of competent E. coli cells is shown in Table 4. Primers used for PCR for Ser120Cys GrUAXS mutant are shown in Table 5. Kits used for plasmid isolation and PCR product purification are shown in Table 6. Buffers used for SDS-PAGE and PCR are shown in Table 7. Buffers prepared for the enzyme purification, storing the enzymes, TLC analysis and HPLC analysis are shown in Table 8. Columns used for purification, gel filtration and HPLC analysis are shown in Table 9. Gels used for SDS-PAGE are shown in Table 10. Gel markers and stain used for SDS-PAGE are shown in Table 11. Enzymes used for the research are shown in Table 12. Filters used for filtration and concentration are shown in Table 13. Equipment used in the research is shown in Table 14.

Table 1. The chemicals used for the research.

Chemicals	**Company/Institution**
(Double) distilled water (dH_2O and ddH_2O)	the Institute of Biotechnology and Biochemical Engineering, TU Graz
1,4-Dithiothreitol (DTT, >99%)	Carl Roth GmbH (Karlsruhe, Germany)
2,2',2",2"'-(Ethane-1,2-diyldinitrilo)tetraacetic acid (EDTA, >99%)	Sigma-Aldrich (St. Louis, USA)
2-Amino-2-hydroxymethyl-propane-1,3-diol (Tris, > 99.9%)	Carl Roth GmbH (Karlsruhe, Germany)
Acetic acid (HAc, 96%)	Sigma-Aldrich (St. Louis, USA)
Acetonitrile (ACN, >99.9%)	Chem-Lab (Zedelgem, Belgium)
Agar-agar, granulated	Carl Roth GmbH (Karlsruhe, Germany)
Agarose, granulated	PeqLab VWR (Radnor, USA)
Ampicillin sodium salt (Amp, >97%)	Carl Roth GmbH (Karlsruhe, Germany)
B-PER™ Bacterial Protein Extraction Reagent	Thermo Fisher Scientific (Waltham, USA)

Table 1. The chemicals used for the research (continuation).

Chemicals	**Company/Institution**
Calcium chloride ($CaCl_2$, >93%)	Sigma-Aldrich (St. Louis, USA)
D-(+)-Glucose (Glc, >99%)	Carl Roth GmbH (Karlsruhe, Germany)
Desthiobiotin (>98%)	Sigma-Aldrich (St. Louis, USA)
Deuterium oxide (D_2O, 99.8%)	Eurisotop (Saint-Aubin, France)
D-Glucuronic acid methyl ester (> 96 %)	Carbosynth (Newbury, UK)
Dipotassium phosphate (K_2HPO_4, >99%)	E. Merck KG (Darmstadt, Germany)
dNTP Mix (10 mM)	Thermo Fisher Scientific (Waltham, USA)
Ethanol (96%)	Carl Roth GmbH (Karlsruhe, Germany)
Glycerol (>98 %)	Carl Roth GmbH (Karlsruhe, Germany)
Hydrogen chloride (HCl, > 99 %)	Sigma-Aldrich (St. Louis, USA)
Imidazol (≥99 %)	Carbosynth (Newbury, UK)
Isopropyl- β-D-thiogalactopyranoside (IPTG, >99 %)	
Magnesium chloride ($MgCl_2$, > 98.5 %)	Carl Roth GmbH (Karlsruhe, Germany)
Methanol (>99.9 %)	Carl Roth GmbH (Karlsruhe, Germany)
Nicotinamide adenine dinucleotide, oxidized form (NAD^+ >98%)	Carl Roth GmbH (Karlsruhe, Germany)
Nicotinamide adenine dinucleotide, reduced form (NADH, >98%)	Carl Roth GmbH (Karlsruhe, Germany)
Peptone from casein	Carl Roth GmbH (Karlsruhe, Germany)
Phosphoric acid (H_3PO_4, 85 %)	Sigma-Aldrich (St. Louis, USA)
Potassium chloride (KCl, >99,5 %)	Carl Roth GmbH (Karlsruhe, Germany)
Potassium dihydrogen phosphate (KH_2PO_4, >99.5%)	E. Merck KG (Darmstadt, Germany)
Potassium hydroxide (KOH, 85%)	Carl Roth GmbH (Karlsruhe, Germany)

Table 1. The chemicals used for the research (continuation).

Chemicals	**Company/Institution**
Sodium chloride (NaCl, >99.5%)	Carl Roth GmbH (Karlsruhe, Germany)
Sodium dihydrogen phosphate (NaH_2PO_4, >98 %)	Carl Roth GmbH (Karlsruhe, Germany)
Sodium hydroxide (NaOH, 99 %)	Carl Roth GmbH (Karlsruhe, Germany)
Sodium pyruvate (NaPyr > 99%)	Sigma-Aldrich (St. Louis, USA)
Tetrabutylammonium bromide (TBAB, > 99%)	Carl Roth GmbH (Karlsruhe, Germany)
UDP-4-keto-pentose	Prepared at the Institute of Biotechnology and Biochemical Engineering, TU Graz
UDP-D-galacturonic acid (UDP-GalA)	the Institute of Biotechnology and Biochemical Engineering, TU Graz
UDP-D-glucuronic acid (UDP-GlcA)	Carbosynth (Newbury, UK)
UDP-Xylose (UDP-Xyl)	the Institute of Biotechnology and Biochemical Engineering, TU Graz
UDP-α-D-glucose (UDP-α-Glc)	the Institute of Biotechnology and Biochemical Engineering, TU Graz
Yeast extract	Carl Roth GmbH (Karlsruhe, Germany)

Table 2. Media used for the transformed *E. coli* growth.

Medium	**Composition**
Lysogeny Broth (LB) medium	10 g/L (1 % w/v) peptone or tryptone 10 g/L (1 % w/v) NaCl 5 g/L (0.5 % w/v) yeast extract
Terrific Broth (TB) medium	10 g/L (1 % w/v) peptone or tryptone 10 g/L (1 % w/v) NaCl 5 g/L (0.5 % w/v) yeast extract 20% v/v Phosphate buffer (0.17 M KH_2PO_4, 0.72 M K_2HPO_4)
S.O.C. Medium	Thermo Fisher Scientific (Waltham, USA)

All media were sterilized by autoclave at 121 °C and 1 bar for 15 min. Agar plates were prepared with 15 g/L agar-agar, 50 μg/mL of ampicillin or kanamycin.

Table 3. *E. coli* strains used for transformation and expression.

Bacterial strains	**Company**
E. coli BL21(DE3)	the Institute of Biotechnology and Biochemical Engineering, TU Graz
E. coli BL21(DE3) LEMO21	the Institute of Biotechnology and Biochemical Engineering, TU Graz
E. coli NEB5α	New England Biolabs (Ipswich, USA)

Table 4. Plasmid used for transformation of competent *E. coli* cells.

Plasmid	**Company**
pET28a_GrUAXS	the Institute of Biotechnology and Biochemical Engineering, TU Graz

Table 5. Primers used for PCR for Ser120Cys GrUAXS mutant.

Primers	**Company**
5'-GTTAGCTTTAGCACCTGCGAAACCTACGGTCGT-3' forward	Sigma-Aldrich (St. Louis, USA)
5'-ACGACCGTAGGTTTCGCAGGTGCTAAAGCTAAC-3' reverse	Sigma-Aldrich (St. Louis, USA)

Table 6. Kits used for plasmid (Table 4.) isolation and PCR product purification.

Kits	**Company**
ExtractMe Plasmid DNA Kit	BLIRT – DNA Gdansk (Gdansk, Poland)
innuPREP PCR Pure kit	Analytik Jena AG (Jena, Germany)
QIAprep® Spin Miniprep kit	Qiagen (Hilden, Germany)
Wizard® Plus SV Minipreps DNA Purification System	Promega Corporation (Madison, USA)
Wizard® SV Gel and PCR Clean-up System	Promega Corporation (Madison, USA)

Table 7. Buffers used for SDS-PAGE and PCR.

Buffers	**Company**
Coomasie staining solution	50% methanol 10% acetic acid 40% H_2O
Destaining solution	40 % v/v methanol 10 % v/v acetic acid
NuPAGE™ LDS Sample buffer 4x	Thermo Fisher Scientific (Waltham, USA)
NuPAGE™ MOPS Running buffer	Thermo Fisher Scientific (Waltham, USA)
Phusion 5x High Fidelity (HF) buffer	Thermo Fisher Scientific (Waltham, USA)
Q5® 5x reaction buffer	New England Biolabs (Ipswich, USA)
Tango *Dpn*I buffer	Thermo Fisher Scientific (Waltham, USA)

Table 8. Buffers prepared for the enzyme purification, storing the enzymes, TLC analysis and HPLC analysis.

Buffers	**Composition**
D_2O UAXS buffer	50 mM K_2HPO_4/ KH_2PO_4, pD 7.0
D_2O UAXS storage buffer	50 mM K_2HPO_4/ KH_2PO_4, 10% glycerol, pD 7.0
Epimerase buffer	50 mM Na_2HPO_4 1 mM DTT 50 mM NaCl, pH 7.6 (adjusted with NaOH)
GrUAXS storage buffer	50 mM Tris 150 mM NaCl 1 mM DTT 10% Glyerol pH 7.6 (adjusted with HCl)
His-trap binding buffer (A)	100 mM Tris 50 mM NaCl 20 mM imidazole pH 7.0 (adjusted with HCl)
His-trap elution buffer (B)	100 mM Tris 50 mM NaCl 400 mM imidazole pH 7.0 (adjusted with HCl)

Table 8. Buffers prepared for the enzyme purification, storing the enzymes, TLC analysis and HPLC analysis (continuation)

Strep-trap elution buffer (E)	100 mM Tris 150 mM NaCl 2.5 mM desthiobiotin pH 8.0 (adjusted with HCl)
Strep-trap regeneration buffer (R)	100 mM Tris 150 mM NaCl 1 mM HABA pH 8.0 (adjusted with HCl)
Strep-trap washing buffer (W)	100 mM Tris 50 mM NaCl pH 8.0 (adjusted with HCl)
TBAB buffer	20 mM K_2HPO_4/KH_2PO_4 40 mM TBAB pH 5.9 (adjusted with HCl)
TLC eluent solution	50% BuOH 25% acetic acid 25% H_2O
Tymol staining solution	0.5% w/v Thymol 95% v/v ethanol 5% v/v H_2SO_4
UAXS buffer	50 mM K_2HPO_4 / KH_2PO_4 100 mM NaCl pH 7.0 (adjusted with H_3PO_4)
UAXS storage buffer	50 mM K_2HPO_4 / KH_2PO_4 100 mM NaCl 1 mM DTT 10% glycerol pH 7.0
UXS storage buffer	50 mM Tris 100 mM NaCl 1 mM DTT 10% Glycerol pH 8

To adjust the pH of the buffers, HCl, H_3PO_4, NaOH or KOH were used. All buffers were filtered using a 0.45 μm cellulose acetate filter.

Table 9. Columns used for purification, gel filtration and HPLC analysis.

Columns	**Company**
HisTrap HP 5 mL	GE Healthcare Life Sciences (Chicago, USA)
Kinetex® 5 μm C18 100 Å, 50 x 4.6 mm	Phenomenex (Torrance, USA)
Kinetex® 5 μm EVO C18 100 Å, 150 x 4.6 mm	Phenomenex (Torrance, USA)
StrepTrap™ HP 5 mL	GE Healthcare Life Sciences (Chicago, USA)
Superdex G-10 size-exclusion column	GE Healthcare Life Sciences (Chicago, USA)

Table 10. Gels used for SDS-PAGE.

Gels	**Company**
NuPAGE™ Bis-Tris Mini Protein Gels, 10 or 15-well	Thermo Fisher Scientific (Waltham, USA)

Table 11. Gel markers and stain used for SDS-PAGE.

Gel markers and stains	**Company**
InstantBlue™ Coomassie Protein Stain	Expedeon (Cambridge, UK)
PageRuler™ Prestained Protein Ladder	Thermo Fisher Scientific (Waltham, USA)

Table 12. Enzymes used for the research.

Enzymes	**Company**
Alcohol oxidase for methanol determination	Sigma-Aldrich (St. Louis, USA)
DpnI restriction enzyme	Thermo Fisher Scientific (Waltham, USA)
Formaldehyde dehydrogenase	Sigma-Aldrich (St. Louis, USA)
Glucuronic acid kinase (GlcAK) wild-type enzyme	the Institute of Biotechnology and Biochemical Engineering, TU Graz

Table 12. Enzymes used for the research (continuation).

GrUAXS wild-type enzyme	the Institute of Biotechnology and Biochemical Engineering, TU Graz
Inorganic pyrophosphatase (iPPase) wild-type enzyme	the Institute of Biotechnology and Biochemical Engineering, TU Graz
Pyruvate kinase	Sigma-Aldrich (St. Louis, USA)
Q5® High-Fidelity DNA Polymerase	New England Biolabs (Ipswich, USA)
UAXS wild-type enzyme	the Institute of Biotechnology and Biochemical Engineering, TU Graz
UGAepi wild-type enzyme	the Institute of Biotechnology and Biochemical Engineering, TU Graz
UDP-glucose pyrophosphorylase (UGPase) wild-type enzyme	the Institute of Biotechnology and Biochemical Engineering, TU Graz
UXS wild-type enzyme	the Institute of Biotechnology and Biochemical Engineering, TU Graz

Table 13. Filters used for filtration and concentration.

Filters	**Company**
Vivaspin 2, 10 kDa MWCO	Sartorius (Göttingen, Germany)
Vivaspin 20, 30 kDa MWCO	Sartorius (Göttingen, Germany)
Vivaspin 500, 10 kDa MWCO	Sartorius (Göttingen, Germany)
Whatman™ Cellulose Acetate Membrane 0.45 μm	GE Healthcare Life Sciences (Chicago, USA)
Whatman™ Syringe Filters 0.45 μm	GE Healthcare Life Sciences (Chicago, USA)

Table 14. Equipment used in the research.

Instrument	**Company**
5424R Centrifuge	Eppendorf AG (Hamburg, Germany)
5810R Centrifuge A-4-62-MTP Rotor	Eppendorf AG (Hamburg, Germany)
691 pH Meter	Metrohm (Herisau, Switzerland)
ÄKTA FPLC system	GE Healthcare Life Sciences (Chicago, USA)
ÄKTAprime Plus	GE Healthcare Life Sciences (Chicago, USA)
Laminar BioAir AURA-2000 M.A.C.	EuroClone S.p.A. (Milan, Italy)
Certomat BS-1 Shaking Incubator	Sartorius (Göttingen, Germany)
CO8000 Cell Density Meter	Biochrom WPA (Cambridge, UK)
Nanodrop (DS-11 Spectrophotometer)	DeNovix Inc. (Wilmington, USA)
Entris® Laboratory Balance	Sartorius (Göttingen, Germany)
Mini-Sub Cell GT System for SDS-PAGE	Bio-Rad Laboratories Inc. (Hercules, USA)
MP-300V Power Supply for SDS-PAGE	Major Science Co. LTD. (Saratoga, USA)
Shimadzu® HPLC-20	Shimadzu Corporation (Kiyamachi-Nijo, Japan)
Sorvall® Evolution™ RC Superspeed Centrifuge	Thermo Fisher Scientific (Waltham, USA)
ThermoMixer® Comfort	Eppendorf AG (Hamburg, Germany)
TM 01 Vortex Mixer	Retsch GmbH (Haan, Germany)
Varian INOVA 500-MHz NMR spectrometer	Agilent Technologies (Santa Clara, USA)
Varioklav® Laboratory Autoclave	Thermo Fisher Scientific (Waltham, USA)
Vibra-Cells Processor VCX130 ultrasound	Sonics & Materials Inc. (Newtown, USA)
DU®800 Spectrophotometer	Beckman Coulter (Brea, USA)
ZWY-B3222 Orbital Floor Shaker	Labwit Scientific (Victoria, Australia)

3.2 METHODS

3.2.1 Synthesis of UDP-GlcA methyl ester

Gene expression, transformed E. coli strains cultivation and cell extract preparation

The enzymes used in the synthesis of UDP-GlcA methyl ester were GlcAK (pET17b_GlcAK; Ampicilin), UGPase (pET30_UGPase, Kanamycin) and iPPase (pET_STRP3_iPPase, Kanamycin). Expression strain *E. coli* BL21 (DE3) was previously transformed with pET30_UGPase and pET_STRP3_iPPase plasmids while *E. coli* BL21 (DE3) LEMO21 was transformed with pET17b_GlcAK.

The pre-cultures of transformed *E. coli* strains [BL21 (DE3) or BL21 (DE3) LEMO21] were prepared by taking 10 μL of their glycerol stocks and transferring it into 10 mL of sterile LB medium with corresponding antibiotic in 50 mL tube and let grow at 37 °C (120 rpm) overnight. After that, main cultures were prepared in baffled flasks (1000 mL) with 250 mL of sterile LB medium with corresponding antibiotic, by adding inoculum (the pre-culture, 2 mL) and cultivation at 37 °C (120 rpm) until optical density (OD) at 600 nm reached 0.8-0.9. Then expression of the enzymes was induced by addition of 0.2 or 0.5 mM IPTG (UGPase and iPPase, and GlcAK, respectively) and the suspension were incubated at 18 °C (120 rpm) overnight.

The *E. coli* cells containing the expressed enzyme were harvested by centrifugation at 5000 rpm and 4 °C for 20 min (Sorvall® Evolution™ RC Superspeed Centrifuge, Thermo Fisher Scientific, Waltham, USA). The supernatant was decanted and the cell pellets were resuspended in 5 mL of His-trap binding buffer (A) (UGPase, His-tag) or 5 mL of Strep-trap washing buffer (W) (iPPase and GlcAK, Strep-tag).

In order to disrupt the cell walls, the resuspended cells were sonicated under following conditions: 7 min, 2 *sec on* – 5 *sec off* cycles and the amplitude of 60 % (the distance between horn's vibrating surface position in the horn's fully extended and fully contracted states, measured in microns; Vibra-Cells Processor VCX130, Sonics & Materials Inc., Newtown, USA). The sonication was performed in a plastic beakers with a stirring-bar inserted. The beakers were kept on ice during the sonication and stirred at 200 rpm on a magnetic mixer.

The insoluble and soluble fractions of the cells lysate were separated by centrifuging at 15000 rpm and 4 °C for 1 h (5424R Centrifuge, Eppendorf AG, Hamburg, Germany). The supernatant

was taken, filtered through a 45 µm filter (WhatmanTM Cellulose Acetate Membrane 0.45 µm, GE Healthcare Life Science, Chicago, USA) and used in chromatographic purification of the enzymes.

Protein purification by affinity chromatography

The superantant was loaded onto the column (StrepTrap™ HP 5 mL or HisTrap™ HP 5 mL, GE Healthcare Life Sciences, Chicago, USA) connected with ÄKTAprime liquid chromatography device (ÄKTAprime Plus, GE Healthcare Life Sciences, Chicago, USA). iPPase and GlcAK were purified by using Strep-tag purification procedure (Maertens et al., 2015) and UGPase by using His-tag purification procedure, as described elsewhere (Spriestersbach et al., 2015).

Before the supernatant loading, the Strep-tag column was equilibrated with Strep-trap washing buffer (W). After the supernatant loading, Strep-trap washing buffer (W) was used to remove the unbound proteins and then the mobile phase was switched to 100% of Strep-trap elution buffer (E) to elute the desired protein with the Strep-tag. The Strep-trap elution buffer (E) contained desthiobiotinin which has the higher affinity for binding to Strep-Tactin than proteins with fused Strep-tag. Flowthrough fractions, washing fractions and elution fractions and were kept for loading SDS-PAGE gel (see *SDS-PAGE of purified enzymes*).

Before the supernatant loading, the His-tag column was equilibrated with His-trap binding buffer (A). After the loading, unbound proteins were washed out with His-trap binding buffer (A) and 100% of His-trap elution buffer (B) applied to elute the His-tagged protein. The His-trap elution buffer (B) contained a high concentration of imidazole (400 mM) competing with His-tag fused proteins for saturating the metal cations in a column. This competition leads to elution of the His-tag fused proteins. As with Strep-tag, flowthrough, elution fractions and washing fractions and were kept for SDS-PAGE.

The elution fractions of each enzyme taken from the columns were concentrated in Vivaspin tubes (iPPase with MWCO 10 kDa, GlcAK with MWCO 30 kDa, and UGPase with MWCO 50 kDa) and the buffer was exchanged with the storage buffer (50 mM Tris, 100 mM Tris, 1 mM DTT, 10 % glycerol, pH 7.0). The concentrations of enzymes were measured on Nanodrop (DS-11 Spectrophotometer/Fluorometer Series, Wilmington, USA) at 280 nm and the purified proteins were frozen with liquid nitrogen before storage at -20 °C.

SDS-PAGE of purified enzymes and staining

The SDS-PAGE was performed to check the purity of the separated proteins. The samples were prepared by taking 10 µL of the sample and mixing it with 10 µL NuPAGE™ sample buffer, 16 µL ddH_2O and 4 µL DTT (1 M) solution. The prepared samples were incubated at 95 °C for 5 min to heat denature the proteins before loading (10 µL) them to NuPAGE™ Bis-Tris gel. The PageRuler™ Prestained Protein Ladder was used as a standard (5 µL). The running conditions were 130 V for 90 min in NuPAGE™ MOPS buffer. After the SDS-PAGE was done, the gel was put to stain into the Commasie staining solution (50 % methanol, 10 % acetic acid, 40 % H_2O) overnight. To destain the gel, it was put into the destaining solution (40 % methanol, 10 % acetic acid).

Preparation of substrate for SDRs

(1) Enzymatic phosphorylation of GlcA methyl ester

The enzymatic phosphorylation of GlcA methyl ester was carried out in a 50 mM Tris-HCl buffer (pH 8.0) in a total volume of 15 mL at 30 °C. GlcA methyl ester (15 mM), phosphoenolpyruvate (25 mM), $MgCl_2$ (5 mM) and ATP (1 mM) were dissolved in 10 mL of 50 mM Tris-HCl buffer and the pH of resulting mixture was adjusted to 8.0 with NaOH (0.5 M). Then, 10 U/mL of pyruvate kinase (375 µL, 400 U/mL of stock solution) and 0.55 mg/mL of GlcAK (503 µL, 16.4 mg/mL stock solution) were added into the reaction mixture and the total volume of the mixture was brought to 15 mL by 50 mM Tris-HCl buffer, pH 8.0.

The phosphorylation progress was followed by thin layer chromatography (TLC; Merck, Silica gel 60, 0.063-0.200 mm). Sample were withdrawn immediately after the reaction started and then after 1.0 and 16.0 h. The samples for TLC were prepared by mixing 15 µL of the sample from the phosphorylation reaction mixture with 15 µL of methanol (99%) and incubated for 15 min at room temperature before centrifugation at 15000 rpm for 5 min (5424R Centrifuge. Eppendorf, AG, Hamburg, Germany). Obtained supernatant was spotted three times on TLC gel (each drop of 2 µL) while GlcA methyl ester standard was spotted only once on TLC gel (2 µL). The TLC run for 30-40 min in a TLC eluent (50% buthanol, 25% acetic acid, 25% H_2O) as a mobile phase. The plates were dried and stained in a tymol solution (0.5% w/v tymol, 95% v/v ethanol, 5% v/v H_2SO_4) then heat dried until the spots were visible.

(2) Enzymatic nucleotidyl-transfer reaction of GlcA methyl ester-1-P

The enzymes from the phosphorylation mixture were removed by heating the mixture up to 90 °C for 2 min and centrifuged at 15000 rpm and +4 °C for 10 min (5810R Centrifuge A-4-62-MTP Rotor, Eppendorf AG, Hamburg, Germany). To obtained supernatant 40 mM of UTP was added and the pH of resulting mixture was adjusted to 8.0 with NaOH (0.5 M) before starting the enzymatic nucleotidyl-transfer reaction by adding UGPase (0.4 mg/mL) and iPPase (0.2 mg/mL).

Progress of the nucleotidyl-transfer reaction was followed by using HPLC method (see below). The samples for HPLC analysis were taken from the reaction mixture after 1.0, 2.0 and 16.0 h and prepared by mixing 25 µL of withdrawn solution with 25 µL of methanol (99%). The samples were incubated at room temperature for 30 min and centrifuged at 15000 rpm for 15 min (5424R Centrifuge, Eppendorf AG, Hamburg, Germany). Kinetex® column (5 µm C18 100 A, 50 x 4.6 mm; Shimadzu Corporation, Kiyamachi-Nijo, Japan) and HPLC system (Shimadzu® HPLC-20, Shimadzu Corporation, Kiyamachi-Nijo, Japan) with UV/Vis detector (262 nm) were used. The mobile phase was a combination of 5% of acetonitrile and 95 % of TBAB buffer) with flow rate of 2 ml/min at 45 °C. UDP-GlcA was run as a standard.

(3) Isolation, purification and identification of UDP-GlcA methyl ester

The enzymes from the nucleotidyl-transfer reaction mixture (see 2) were removed by using Vivaspin 10 kDa MWCO filter. 10 U/mL of calf-intestine alkaline phosphatase (14 µL, 10000 U/ml of CIP stock solution) was added into the reaction mixture and the mixture was incubated at 30 °C for 16 h. The CIP was removed by ultrafiltration (Vivaspin 10 kDa MWCO) and the UDP-GlcA methyl ester in resulting filtrate was divided into tree portions and subjected to precipitation under three different conditions, as follows. The first beaker contained the filtrate (2.0 mL), five-fold volumes of ethanol (10 ml, 96 % ethanol stock solution), 480 µL NaOH (200 mM, pH 7.0) and resulting mixture was incubated at +4 °C for 72 h without shaking. The second beaker contained the filtrate (2.0 mL) and five-fold volume of ethanol (10 ml, 96 % ethanol stock solution), and the third beaker contained the filtrate (1.5 mL), five-fold volumes of ethanol (7.5 ml, 96 % ethanol stock solution), and sodium acetate (1 mL, 100 mM). Apart from the filtrate, the ethanol only containg mixture (beaker 2) and the ethanol and sodium acetate containing mixture (beaker 3) were incubated at -20 °C for 72 h withou shaking. Resulting precipitate from beakers 1 - 3 was recovered by centrifugation at 4000 rpm and +4 °C for 30 min (5810R Centrifuge A-4-62-MTP Rotor, Eppendorf AG, Hamburg, Germany).

The resulting powder containing UDP-GlcA methyl ester was air dried (for about 15 min) at room temperature, weighed, transfered into the new 50 mL tube and stored at -20 °C as a solid. The supernatant and the precipitate (dissolved in ddH_2O) separately were analyzed by HPLC method [see under (2)].

Identification od UDP-GlcA methyl ester by ^{1}H-NMR

Precipitate containing UDP-GlcA methyl ester obtained after air drying was dissolved directly in 700 µL D_2O to achieve a 50 mM solution and analyzed by ^{1}H-NMR (Varian INOVA 500-MHz NMR, Agilent Technologies, Santa Clara, USA).

3.2.2 Preparation of UXS, UAXS and UGAepi and their activity towards UDP-GlcA and UDP-GlcA methyl ester

(1) Gene expression

UXS (pET26a_UXS) and UAXS (pET26a_UAXS) were available as glycerol stocks of transformed *E. coli* (available at the Institute of Biotechnology and Biochemical Engineering, TU Graz) and UGAepi was available as purified enzyme (at the Institute of Biotechnology and Biochemical Engineering, TU Graz). Expression protocol for UXS (pET26a_UXS) and UAXS (pET26a_UAXS) was the same as described previously for UGPase and iPPase (see chapter 3.2.1; *Gene expression, transformed* E. coli *strains cultivation and cell extract preparation*).

(2) Protein purification by affinity chromatography

Both, UXS and UAXS, are His-tag proteins and were purified by following the same protocol as for UGPase (see chapter 3.2.1; *Protein purification by affinity chromatography*). In addition, purified dimer UXS was separated on Superdex G-10 size-exclusion column (GE Healthcare Life Sciences, Chicago, USA) by using 50 mM Tris buffer (1 mM DTT, 100 mM NaCl, pH 8.0). The fractions were merged and concentrated in Vivaspin 30 kDa MWCO.

(3) Kinetic studies on UAXS, UXS and UGAepi with two substrates - UDP-GlcA and UDP-GlcA methyl ester

UXS and UAXS reactions were performed in 50 mM Tris-HCl buffer (pH 8.0 for UXS and pH 7.0 for UAXS) in a total volume of 150 µL at room temperature. The enzymes were tested with their natural substrate UDP-GlcA and with UDP-GlcA methyl ester. The UXS reaction was tested with 1 mg/mL and 0.3 mg/ml of UXS. The UAXS reation was performed with 2 mg/mL of UAXS. 2 mM of each substrate was mixed together with 0.1 mM of NAD^+ in the 50 mM Tris-HCl buffer. The reaction was started by adding the enzyme.

UGAepi reaction was performed in the 50 mM epimerase buffer (pH 7.6) in a total volume of 150 µL at room temperature with UDP-GlcA and UDP-GlcA methyl ester. The reaction was probed with 0.07 mg/mL and 0.0035 mg/mL of UGAepi. 1 mM of substrate was mixed together with 0.1 mM of NAD^+ in the 50 mM epimerase buffer, pH 7.6. The reaction was started by adding the enzyme.

Products of above described reactions were separated, identified and quantified by HPLC method [see chapter 3.2.1; *Preparation of substrate for SDRs, (2)*]. The samples for the HPLC analysis were taken from reaction mixtures at different time points (0, 5, 10, 15, 30, 45, 60 and 90 min).

Additionally, the UXS and UAXS reactions samples from 60 min and 90 min time-points were analyzed by another HPLC method (Shimadzu® HPLC-20, Shimadzu Corporation, Kiyamachi-Nijo, Japan) at 262 nm in Kinetex® column (5 µm EVO C18 100 Å, 150 x 4.6 mm). Here, as a mobile phase the combination of 3% methanol and 97% TBAB buffer was used with 1 ml/min flow rate at 45 °C.

Identification of products-UDP-Api, UDP-Xyl and UDP-GalA by ^{1}H-NMR

The enzymes were rebuffered against 50 mM D_2O UXS buffer (K_2HPO_4/ KH_2PO_4), pH 7.0 and the compounds (see below) used for the reactions dissolved in D_2O. So, KH_2PO_4 was dissolved in 5 mL of D_2O and K_2HPO_4 was dissolved in 5 mL of D_2O to achieve 50 mM of each. K_2HPO_4 solution was titrated by KH_2PO_4 until pH reached either 6.6 (pD 7.0, UXS) or 7.6 (pD 8.0, UAXS) for UXS and UAXS reactions. For the UGAepi reaction pH of K_2HPO_4/ KH_2PO_4 buffer was adjusted to 7.2 (pD 7.6). The pH electrode (691 pH Meter, Metrohm, Herisau, Switzerland) used for the K_2HPO_4/ KH_2PO_4 buffer wirh different pD was equilibrated in D_2O for 30 min before it was used for adjusting the pD following the equation pD = pH + 0.4. Rebuffering of the enzymes in a prepared D_2O K_2HPO_4/ KH_2PO_4 buffers was performed by using the Vivaspin

10 kDA MWCO (previously rinsed with D_2O). The enzymes were first concentrated to a volume below 100 μL, and then three-fold volumes of D_2O K_2HPO_4/ KH_2PO_4 buffer were added and the enzymes were concentrated again to volume of approximately 100 μL.

Then, enzyme reactions (UXS, UAXS and UGAepi) were performed in order to obtain corresponding products to be identified by ^{1}H-NMR. The reaction conditions for UXS and UAXS were as described previously *(3)* but scaled up to 700 μL and performed in D_2O. In UGAepi reaction reaction mixture 2 mM of UDP-GlcA methyl ester and 0.1 mM of NAD^+ were mixed together in D_2O K_2HPO_4/ KH_2PO_4 buffer. By the addition of 1 mg/mL of enzyme, the volume was brought to 700 μL and the reaction was started. All the reactions were running for 90 min at romm temperature without shaking and the samples were analyzed by HPLC method [see 3.2.1; *Preparation of substrate for SDRs*, (2)].

The enzymes from reaction mixture were removed by ultrafiltration (Vivaspin 10 kDa MWCO filters) and the supernatants were analyzed by using ^{1}H-NMR (Varian INOVA 500-MHz NMR, Agilent Technologies, Santa Clara, USA).

Monitoring the methanol formation during UDP-GlcA methyl ester conversion by UXS, UAXS and UGAepi

Possible methanol formation during UDP-GlcA methyl ester conversion by UXS, UAXS and UGAepi was followed at 340 nm (spectrophotometer DU®800 Spectrophotometer, Beckman Coulter, Brea, USA). The assay was based on alcohol oxidase reaction with methanol (possibly formed by hydrolysis of UDP-GlcA methyl ester bond) producing formaldehyde, which is then converted to formate by formaldehye dehydrogenase (Vlnet, 1987). In this reaction NADH is produced and can be followed at 340 nm (Vlnet, 1987). 1 mol of NADH corresponds to 1 mol of produced methanol in conversion of UDP-GlcA methyl ester.

The UXS, UAXS and UGAepi reactions contained so called enzymic reagent (2.5 mM NAD^+ and 0.5 U/mL formaldehyde dehydrogenase in 0.1 M Na_2HPO_4/KH_2PO_4 phosphate buffer pH 7.6; 30-fold diluted in the final mixture), then 1.6 mM of the substrate (UDP-GlcA or UDP-GlcA methyl ester), and alcohol oxidase (1 U/ml). The reactions were started by addition of 0.3 mg/mL of UXS, or 2 mg/mL of UAXS, or 0.0035 mg/mL of UGAepi and final volume of each reaction mixture was 530 μL. Every compound and enzyme were dissolved in 0.1 M phosphate (Na_2HPO_4/KH_2PO_4) buffer (pH 7.6). The reactions were carried out at 30 °C over 40 min. The absorbance was recorded every 7.7 s. The phosphate buffer was used as a blank for the

spectrofotometer. The blank reactions included all the same components, but without the enzymes (UXS, UAXS and UGAepi).

In order to make the calibration curve the following methanol solutions were prepared from the methanol stock (25 M): 0, 3, 9, 15, 21, 30, 45, 60 and 90 mM. The methanol solutions were added to so called the enzymic reagent (see above) and reaction was started by adding 1 U/mL of alcohol oxidase only.

3.2.3 Production of a novel bacterial UDP-Apiose/UDP-Xylose synthase (GrUAXS) and its mutant

(1) Transformation of pET28a_GrUAXS into E. coli BL21 (DE3) LEMO21 cells

E. coli BL21 (DE3) LEMO21 cells were transformed with pET28a_GrUAXS (Table 4).

3 μL of plasmid (260 ng/μL of pET28a_GrUAXS stock solution, stored in a 1.5 mL tube at -20 °C) was mixed with 50 μL of *E. coli* BL21 (DE3) LEMO21 competent cells in 1.5 mL tube and incubated on ice for 30 min. The heat-shock was given at 42 °C for 10 s and the suspension was further incubated on ice for 2 min. 500 μL of S.O.C Medium was added to the tube containing pET28a_GrUAXS and *E. coli* BL21 (DE3) LEMO21 and the tube was incubated at 37 °C (120 rpm) for 1 h. After 1 h, the tube was centrifuged at room temperature for 2 min (10000 rpm) and half of the supernatant was discarded. About 250 μL of the suspension left in the tube was resuspended and plated on LB agar plates supplemented with kanamycin and grew at 37 °C for 16 h.

(2) Gene expression

Two approaches for gene encoding GrUAXS expression were tried in order to obtain a reasonable yield of the proteine. The first approach was the standard expression protocol as described for UGPase and iPPase (see chapter 3.2.1; *Gene expression, transformed E. coli strains cultivation and cell extract preparation*). Pre-cultures of transformed *E. coli* BL21 (DE3) LEMO21were made by picking the single colony from the LB agar plates supplemented with kanamycin instead of using the glycerol stock. One of the pre-cultures was used for plasmid isolation using the ExtractMe Plasmid DNA Kit (BLIRT – DNA, Gdansk, Poland) or Wizard® Plus SV Minipreps DNA Purification System (Promega Corporation, Madison, USA). Concentration of the isolated plasmid was measured on Nanodrop (DeNovix Inc.,

Wilmington, USA) at 260 nm. Part of the suspension (20 μL) was used for determination of isolated plasmid concentration and the plasmid solution was sent for sequencing to LGC Genomics GmBH company (Berlin, Germany). The expression of gene encoding GrUAXS in the second approach was carried out in the same way, but at 30 °C and 250 rpm for 4 h (Smith and Bar-Peled, 2017). The cells containing the expressed GrUAXS were harvested by centrifugation at 5000 rpm (+4 °C) for 20 min (Sorvall® EvolutionTM RC Superspeed, Thermo Fisher Scientific, Waltham, USA).

(3) GrUAXS purification by affinity and size-exclusion chromatography

Given that GrUAXS has the His-tag fused, the protein was purified according to the protocol described previously (see chapter 3.2.1; *Protein purificiation by affinity chromatography*) and afterwards the dimer separated on Superdex G-10 size exclusion column (GE Healthcare Life Sciences, Chicago, USA) previously washed with GrUAXS buffer (50 mM Tris, 150 mM NaCl, 1 mM DTT, pH 7.6). The fractions containing the dimeric protein were collected, merged and concentrated by ultrafiltration (Vivaspin 30 kDa MWCO filter) and rebuffered in GrUAXS storage buffer (GrUAXS buffer with 10% glycerol).

(4) Activity of GrUAXS towards UDP-GlcA

The reaction was carried out by using 0.2 and 5 mg/mL of the enzyme in 50 mM Tris-HCl buffer (pH 8.0), 1 mM of UDP-GlcA (7.5 μL, 20 mM stock solution) and 1 mM of NAD^+ (5 μL , 30 mM stock solution) in a total volume of the reaction mixture of 100 μL at 37 °C. The samples were taken at 0, 5, 10, 15, 30, 45, 60 and 90 min and prepared by mixing 12 μL of the reaction mixture and 28 μL of methanol, incubation over 30 min at room temperature and then centrifuged for 15 min (15000 rpm, +4 °C; 5424R Centrifuge, Eppendorf AG, Hamburg, Germany). Supernatant was analyzed by the HPLC method (see chapter 3.2.2; *(3) Kinetic studies on UAXS, UXS and UGAepi with two substrates - UDP-GlcA and UDP-GlcA methyl ester*).

(5) Mutagenesis, expression optimization, purification and activity of GrUAXS S120C variant

The primers were designed and ordered from Sigma-Aldrich (St. Louis, USA). GrUAXS wild-type enzyme (pET28a_GrUAXS) was used as a template for generating the GrUAXS S120C variant (Table 15.). The primer sequences are given in Table 4. The mutation was introduced

by PCR utilizing a two-stage method (Wang and Malcolm, 1999) with a modified protocol of QuikChangeTM site-directed mutagenesis followed by a DpnI digestion (Wang and Malcolm, 1999). In order to prevent the dimerization of the complementary primers, the initial stage of linear amplification was performed on both primers separately. In the following stage, the actual PCR amplification takes places starting from the newly generated hybrid plasmids, improving the efficiency of the PCR reaction significantly. Table 4 shows the altered PCR reaction set-up. Each PCR mixture contained 20 ng of the template (pET28a_GrUAXS) and 0.2 μM of either reverse or forward primer.

Table 15. PCR reaction set-up for a single PCR reaction with a final volume of the mixture of 50 μL.

Component	**Volume** (μL)
pET28a_GrUAXS (25 ng/μL stock)	0.8
Primer (either forward or reverse, 10 μM stock)	1.0
5x High Fidelity (HF) buffer	10.0
dNTP	1.0
Q5 polymerase (Phusion)	1.0
Double distilled H_2O	36.2

The protocol for running the PCR reactions is shown in Table 16. The linear amplification as the inital stage, including the denaturation, annealing and extension, was repeated for 3 cycles. The PCR mixtures containing primers were merged together and run for 15 more cycles. The annealing temperature in the first three cycles was 55 °C instead of 60 °C. The black rectangle comprises one cycle.

Table 16. Temperature profile and the duration of the steps for PCR reaction.

Step	**Temperature (°C)**	**Time**
Initial duration	98	30 sec
Denaturation	98	10 sec
Annealing	60	15 sec
Extension	72	6 min
Final extension	72	5 min
Hold	10	∞

pET28a_GrUAXS used as a template was digested by adding 1 µL of the restriction endonuclease DpnI (Thermo Fisher Scientific, Waltham, USA) and 6 µL of Tango DpnI buffer (Thermo Fisher Scientific, Waltham, USA) to the PCR mixture containing PCR product and incubated at 37 °C overnight. Wizard® SV Gel (Promega Corporation , Madison, USA) and PCR Clean-up System (Promega Corporation, Madison, USA) were used for additional purification of the PCR product.

7 µL of PCR mixture was used for transformation of 30 µL of chemically competent *E. coli* NEB5α cells. Here the transformation protocol described for LEMO21 with a 30-s heat-shock instead of 10 sec was followed [see 3.2.3; *(1)*]. Then, *E. coli* NEB5α cells cells were plated on kanamycin supplemented LB agar plates and incubated at 37 °C overnight. The pre-cultures of transformants were made by picking six colonies separately and transferring them into 10 mL of sterile LB medium each. The cells were grown overnight at 37 °C (120 rpm). The overnight cultures were used for the plasmid isolation according to plasmid isolation method described for pET28a_GrUAXS [see 3.2.3; *(2)*] and sent for sequencing [see 3.2.3; (2)]. Considering the sequencing results, the desired mutant was obtained and the plasmid used for the transformation of *E. coli* LEMO21 strain (3 µL of plasmid + 50 µL of competent cells). Different expression conditions were tried in order to express the GrUAXS S120C variant (Table 17). The expression protocol for GrUAXS S120C is described in chapter 3.2.1; *Gene expression, transformed E. coli strains cultivation and cell extract preparation*.

Table 17. The expression conditions for GrUAXS S120C variant.

Expression trial	T (°C)	IPTG (mM)	rpm	Kan (µL/mL)	t (h)
1	18	0.1	120	1	18
2	18	0.2	120	1	18
3	30	0.2	250	1	4
4	18	0.5	120	1	18

Trials 1,2 and 4 were chosen for the harvesting and further purification. Before harvesting the cells, 1.5 mL of each suspension (trials 1,2 and 4) was taken and resuspended in B-PER™ Bacterial Protein Extraction Reagent protocol (Thermo Fisher Scientific, Waltham, USA) in order to determine whether the mutant was present in soluble or insoluble fraction of the suspension. By B-PER™ Bacterial Protein Extraction Reagent protocol (Thermo Fisher Scientific, Waltham, USA) the soluble and insoluble fractions were obtained and run on SDS-PAGE (ses 3.2.1; *SDS-PAGE of purified enzymes and staining*). The GrUAXS S120C containing cell were harvested and the cell extract was prepared (see 3.2.1; *Gene expression, transformed E. coli strains cultivation and cell extract preparation*) for His-tag purification with gradient elution (see below). The elution was performed gradually (stepwise) by switching from His-trap binding buffer (A) to 10% His-trap elution buffer (B) followed by 30% His-trap elution buffer (B) and 100% in the end. Each elution step was performed until undesired proteins were washed out. The flowthroughs, washing fractions and fractions from three elution steps were collected. The elution fractions were concentrated with Vivaspin 30 kDa MWCO filter, rebuffered against GrUAXS storage buffer (50 mM Tris, 150 mM NaCl, 1 mM DTT, 10 % glycerol, pH 7.6) and aliquots frozen in liquid nitrogen. All the fractions were analysed by SDS-PAGE (see 3.2.1; *SDS-PAGE of purified enzymes and staining*).

The enzyme activity was tested with 5 mg/mL and 0.3 mg/mL of the enzyme in 50 Mm Tris-HCl buffer (pH 8.0) at 37 °C. UDP-GlcA concentration was 1 mM and NAD^+ concentration was 1 mM. In case of the reaction with 0.3 mg/mL of enzyme, no additional NAD^+ was added to examine the impact of external NAD^+ to the activity of enzyme. The samples from the reaction mixture were taken at 0, 5, 10, 15, 30, 45, 60 and 90 min and analyzed by the HPLC method (see 3.2.2; *(3) Kinetic studies on UAXS, UXS and UGAepi with two substrates - UDP-GlcA and UDP-GlcA methyl ester*).

4. RESULTS AND DISCUSSION

4.1 SYNTHESIS OF UDP-GlcA methyl ester

Given that the focus of the work was studying the decarboxylation mechanisms of UXS and UAXS as well as the rotation step of UGAepi, the first step was to synthesize the substrate analogue for that purpose. UDP-GlcA methyl ester was the interesting one considering that it has the methyl ester moiety which prevents the easy decarboxylation. Figure 8 shows the planned route for the synthesis.

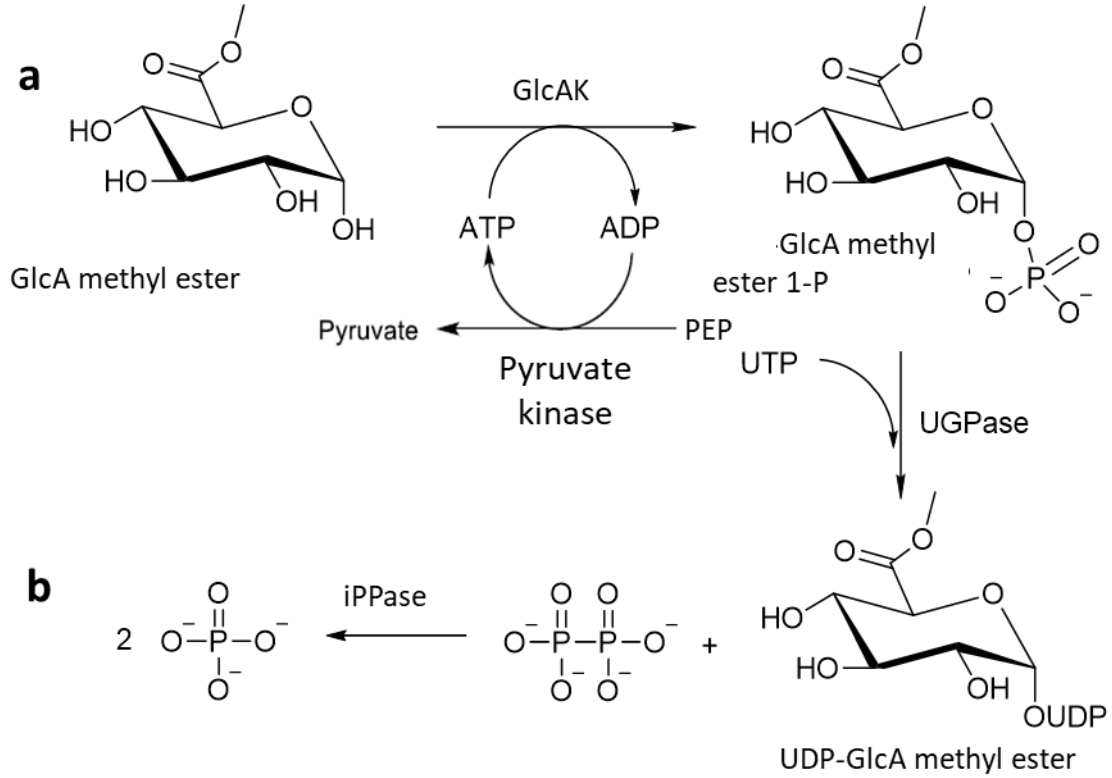

Figure 8. The planned enzymatic route for the synthesis of UDP-GlcA methyl ester. The first step (a) was phosphorylation of GlcA methyl ester to form GlcA methyl ester 1-P. The second step (b) was nucleotidyl transfer from UTP to GlcA methyl ester 1-P to synthesize UDP-GlcA methyl ester. ATP recycling system is also shown. PEP stands for phosphoenolpyruvate.

The synthesis of UDP-GlcA methyl ester was based on the route established and reported previously for synthesizing UDP-GlcA (Pieslinger et al., 2010). Nucleotide sugars in plants can be synthesized *de novo* from UDP-glucose and GDP-mannose (Pieslinger et al., 2010). About 50% of UDP-GlcA in a cell wall is synthesized from UDP-glucose and resembles an important metabolite for NSEs (Pieslinger et al., 2010). In many plants the sugar kinase pathway exists which enables the plants to synthesize NDP sugars by converting the sugar-1-phosphates

produced by kinases (Pieslinger et al., 2010). The sugar-1-kinase transfers γ-phosphoryl group from NTP to a monosaccharide C1 (Pieslinger et al., 2010). One of those kinases is glucuronic acid kinase (GlcAK) selected for UDP-GlcA methyl ester synthesis since GlcA methyl ester is very similar to the natural substrate GlcA. Alongside GlcAK reaction, ATP recycling system was established using phosphoenolpyruvate (PEP) and pyruvate kinase (Cardenas, 1982). The phosphorylation was followed by nucletiodyl transfer reaction using UGPase and iPPase.

SDS-PAGE of purified enzymes

All the enzymes were successfully expressed in *E. coli* BL21 (DE3) LEMO21 strain (see 3.2.1; *Gene expression, transformed* E. coli *strains cultivation and cell extract preparation*).
Figure 9 shows the SDS-PAGE gels after the purification of GlcAK, UGPase and iPPase (see chapter 3.2.1; *Protein purification by affinity chromatography*).

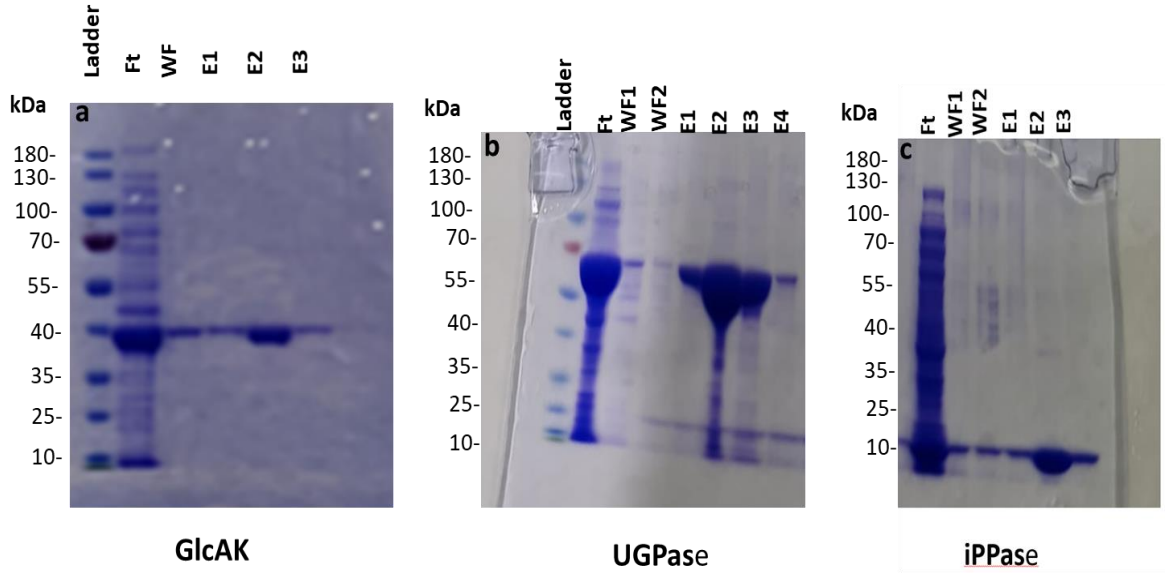

Figure 9. SDS-PAGE gels of the purified GlcAK, UGPase and iPPase used for the synthesis UDP-GlcA methyl ester. The labels show flowthrough (Ft), washing fractions (WF1, WF2), elution fractions (E1, E2, E3) and the molecular mass ladder (Ladder) with corresponding molecular weights in kDa.

The gels show that the enzymes were obtained with their expected molecular weights: : ~39 kDa (GlcAK), ~58 kDa (UGPase) and ~20 kDa (iPPase). All the enzymes were in good purity

and can be recovered from Ft by repeating the purification since it contains a reasonable amount of each enzyme.

Preparation of substrate for SDRs

(1) Enzymatic phosphorylation of GlcA methyl ester

Activity of GlcAK was tested towards natural substrate – GlcA and results of the TLC of the reaction is shown in Figure 10.

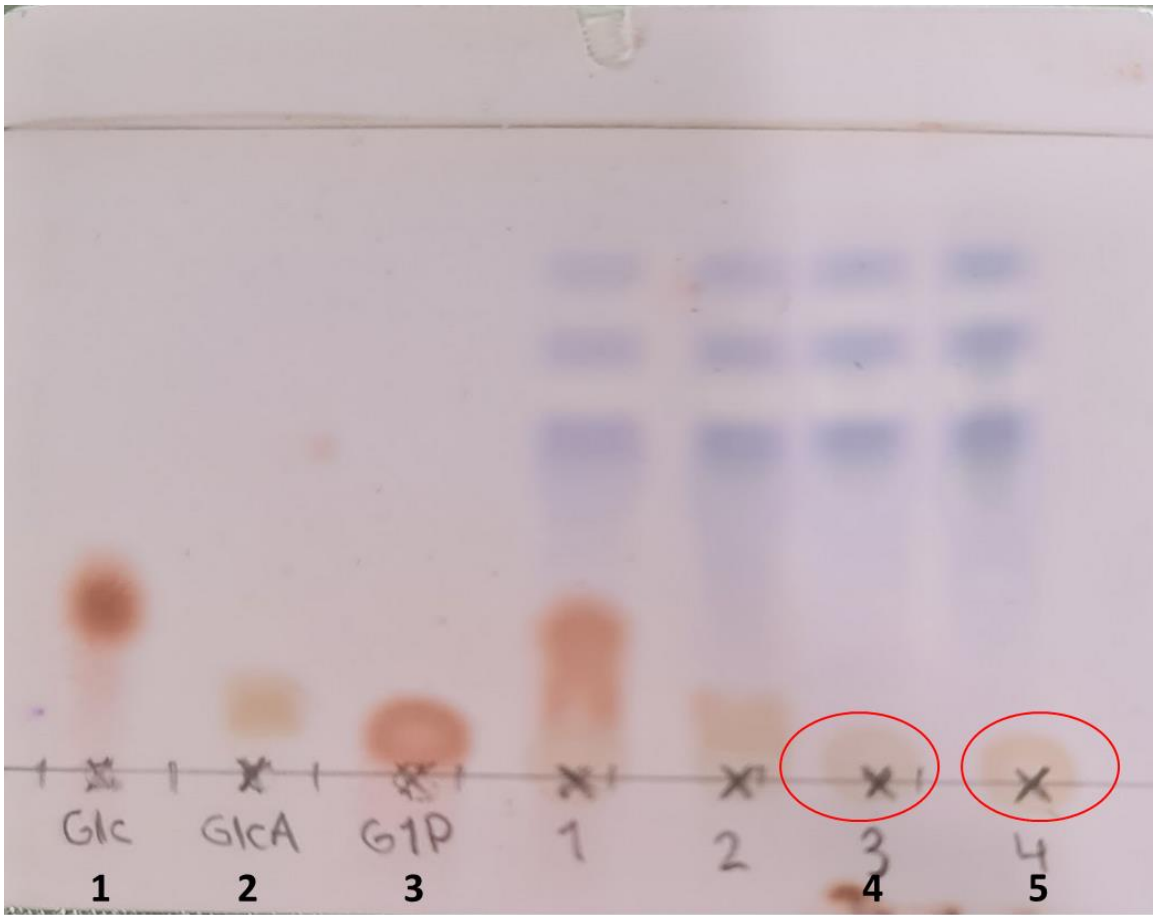

Figure 10. TLC of the reaction catalyzed by GlcAK after 1 h [see 3.2.1; *(1)*]. The product (GlcA 1-P) is labeled with the red circle. As a comparison, glucose (1), GlcA (2) and glucose 1-P (3) are shown. (4) show the reaction of GlcAK with 5 mM of GlcA. (5) shows the reaction with 15 mM of GlcA. The standard is not shown.

The reaction with 15 mM of GlcA gave a better yield of GlcA 1-P (the spot in a red circle is darker). Considering that GlcA methyl ester is not the natural substrate for GlcAK, the investigation was continued with testing the activity of GlcAK with 15 mM of GlcA methyl ester under the same conditions [see 3.2.1; *(1)*]. The TLC analysis of the reaction is shown in Figure 11.

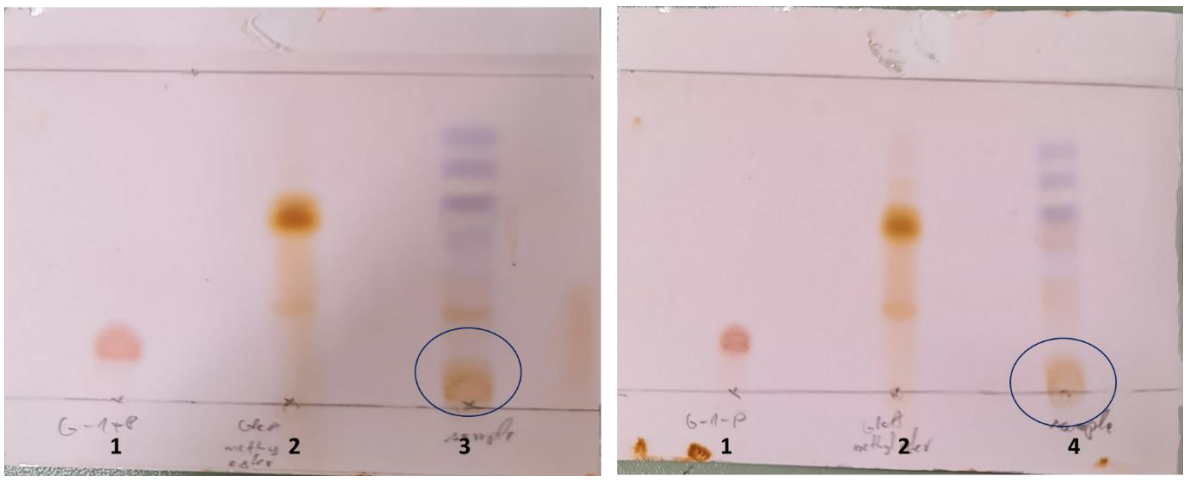

Figure 11. The TLC of the GlcAK reaction with 15 mM GlcA methyl ester. The blue circles indicate the formed GlcA methyl ester 1-P after 1 h (3) and 20 h (4). As comparison, GlcA methyl ester (2) and glucose 1-P (1) are also shown. The standard is not shown.

The substrate was almost fully converted (> 90 %, estimated by comparing the colours of GlcA methyl ester standard and GlcA methyl ester 1-P) after 1 h indicating that the enzyme accepts GlcA methyl ester as its natural substrate. The reaction was scaled-up to 15 mL under the same conditions, except GlcAK which was added in a lower concentration [0.55 mg/mL; see 3.2.1; *(1)*] than in previous experiment. The synthesis route is displayed in Figure 8 (a). The TLC analysis of scaled-up reaction is shown in Figure 12.

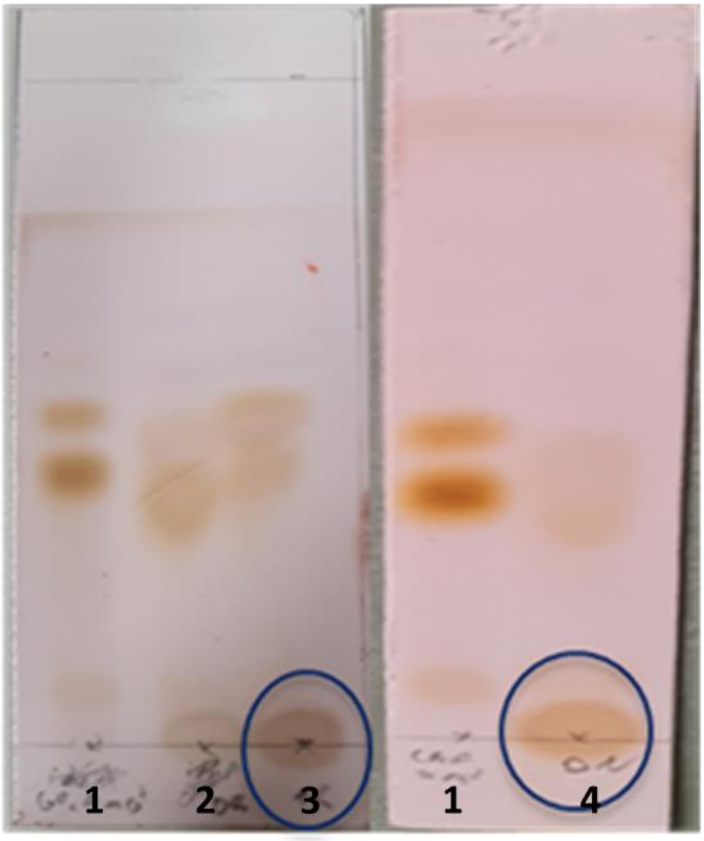

Figure 12. The TLC showing the scaled-up reaction (15 mL) of GlcAK with GlcA methyl ester progress after 0 (2), 1 (3) and 20 h (4). GlcA methyl ester is shown for a comparison (1). GlcA methyl ester 1-P formed after 1 and 20 h in the reaction mixture is labeled with the blue circle.

The reaction worked out with a high conversion efficency of around 90 % after 1 h (estimated by comparing the colours of GlcA methyl ester standard and the product from the reaction mixture). Interestingly, only 0.55 mg/mL of GlcAK led to > 90% conversion of the substrate which is not typical for the kinases in general when the substrate is unnatural (Rapp et al., 2021).

(2) Enzymatic nucleotidyl-transfer reaction of GlcA methyl ester-1-phosphate

After GlcA methyl ester 1-P was produced and the kinase (GlcAK) was removed [see chapter 3.2.1; *(2)*], the next step was a nucleotidyl-transfer reaction catalyzed by UGPase and iPPase. The enzymatic route is shown in Figure 8 (b). The progress of nucleotidyl-transfer reaction was tracked on HPLC by taking the 1, 2 and 24 h samples from that reaction and analyzing them by the HPLC method [see chapter 3.2.1; *(2)*]. Figure 13 shows the HPLC chromatogram of the nucleotidyl-transfer reaction after 24 h.

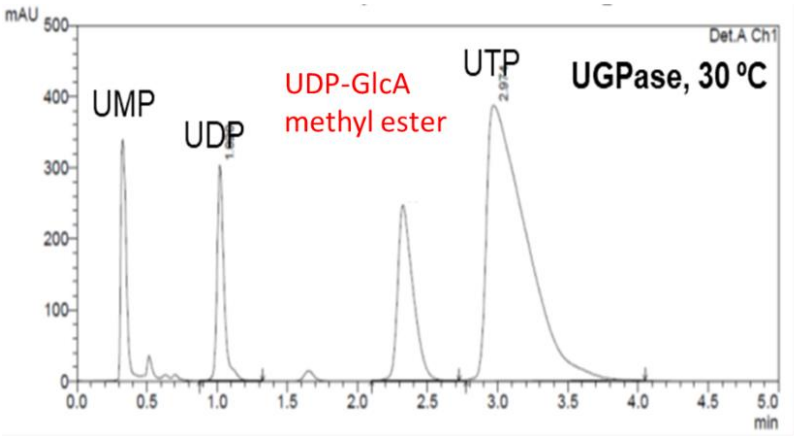

Figure 13. HPLC chromatogram of the UGPase reaction with GlcA methyl ester 1-P after 24 h. The peak coming from UDP-GlcA methyl ester is shown. UMP, UDP and UTP peaks are also shown.

The conversion rate, calculated by integrating the peaks of UTP, UDP and UDP-GlcA methyl ester in the end point of the reaction (24 h), was 17.8 % (data not shown).

(3) Isolation, purification and identification of UDP-GlcA methyl ester

The next step was isolation and purification of the product by running the calf-intestine alkaline phosphatase (CIP) digestion of the nucleotidyl-transfer reaction mixture containing UDP-GlcA methyl ester [see chapter 3.2.1; *(3)*] in order to remove excess of nucleotides (*e.g.* UMP) which could precipitate together with UDP-GlcA methyl ester (see below). The CIP digestion was followed by ethanol precipitation of UDP-GlcA methyl ester [see chapter 3.2.1; *(3)*].

General and widely used method for the downstream processing (DSP) of NDP-sugars is anion exchange chromatography (AEC) followed by size-exclusion chromatography (SEC) (Lemmerer et al., 2016). However, for a large scale biosynthesis AEC and SEC cause the severe problems regarding the costs of the NDP-sugars production and solvent consumption. NDP-sugars can be unstable due to high concentracions of salts as well (Lemmerer et al., 2016). By taking these facts into account, DSP is the bottleneck of the whole NDP-sugar production (Lemmerer et al., 2016). Besides the mentioned classical DSP, an alternative protocol replacing AEC and SEC with ethanol precipitation was reported (Lemmerer et al., 2016). The principle is to create a shield around the phosphate charges of NDP-sugar by monovalent cations (Lemmerer et al., 2016). The role of ethanol is to allow the interactions between phosphates and cations considering its 3-fold lower dielectric constant comparing to water. The commonly

used salt for introducing the monovalent cations in a solution is sodium acetate (Lemmerer et al., 2016). For the puropose of precipitating the UDP-GlcA methyl ester, sodium acetate could not be used since the acetate can hydrolyze the ester bond. On the other hand, sodium hydroxide seemed to be reasonable alternative due to its possibility to neutralize its hydroxide ions and still have monovalent cations in a solution.

The efficiency of the precipitation of UDP-GlcA methyl ester was checked by the HPLC method. Both, the precipitate (dissolved in ddH_2O) and supernatant were checked for each precipitation conditions [see chapter 3.2.1; *(3)*]. Figure 14 shows the HPLC chromatogram of the precipitation reaction of UDP-GlcA methyl ester with sodium hydroxide.

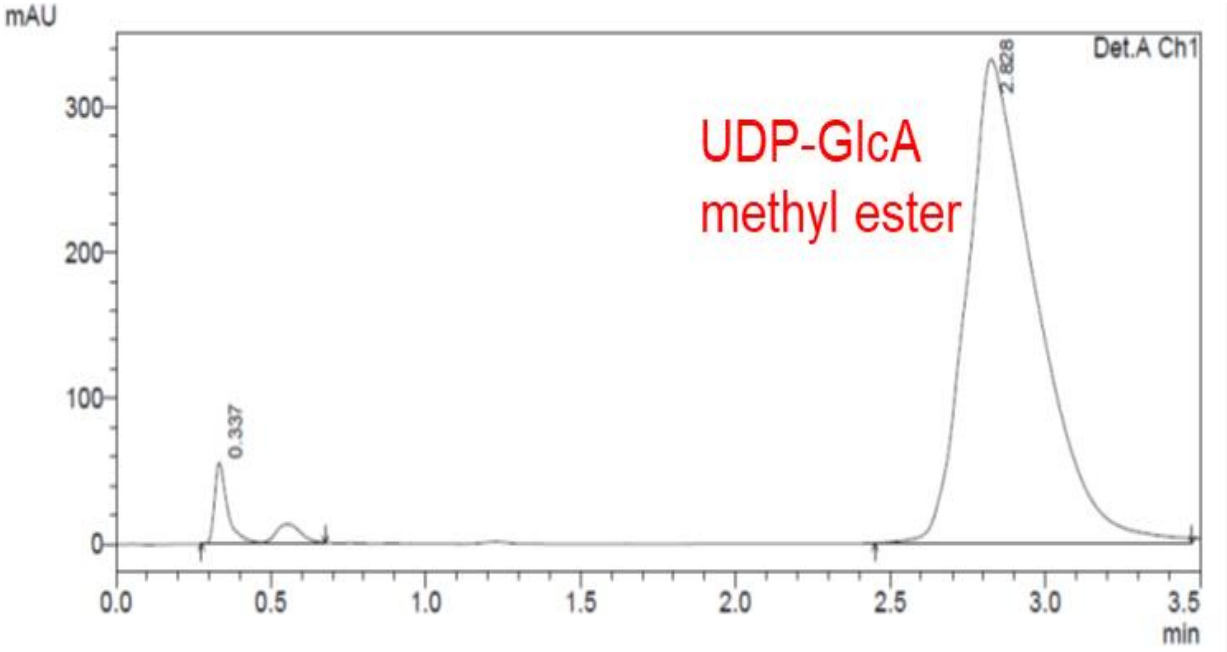

Figure 14. The HPLC chromatogram of the precipitate (dissolved in ddH_2O before the analysis by the HPLC method [see chapter 3.2.1; *(2)*]) obtained with sodium hydroxide and ethanol precipitation. The peak coming from UDP-GlcA methyl ester is shown.

The supernatant did not show any product. The precipitation with only ethanol and with only sodium acetate did not show any product as well (dana not shown). As expected, the precipitation with sodium acetate and ethanol did not work due to hydrolysis of the ester bond. The method with sodium hydroxide was much more efficient with over 96 % purity (obtained by integrating the peaks from HPLC chromatogram) of the product. UDP-GlcA methyl ester was weighed and 11.1 mg of the product was obtained.

Identification od UDP-GlcA methyl ester by ^{1}H-NMR

Further step in this investigation was to confirm that the product still had methyl group by ^{1}H-NMR (Figure 15).

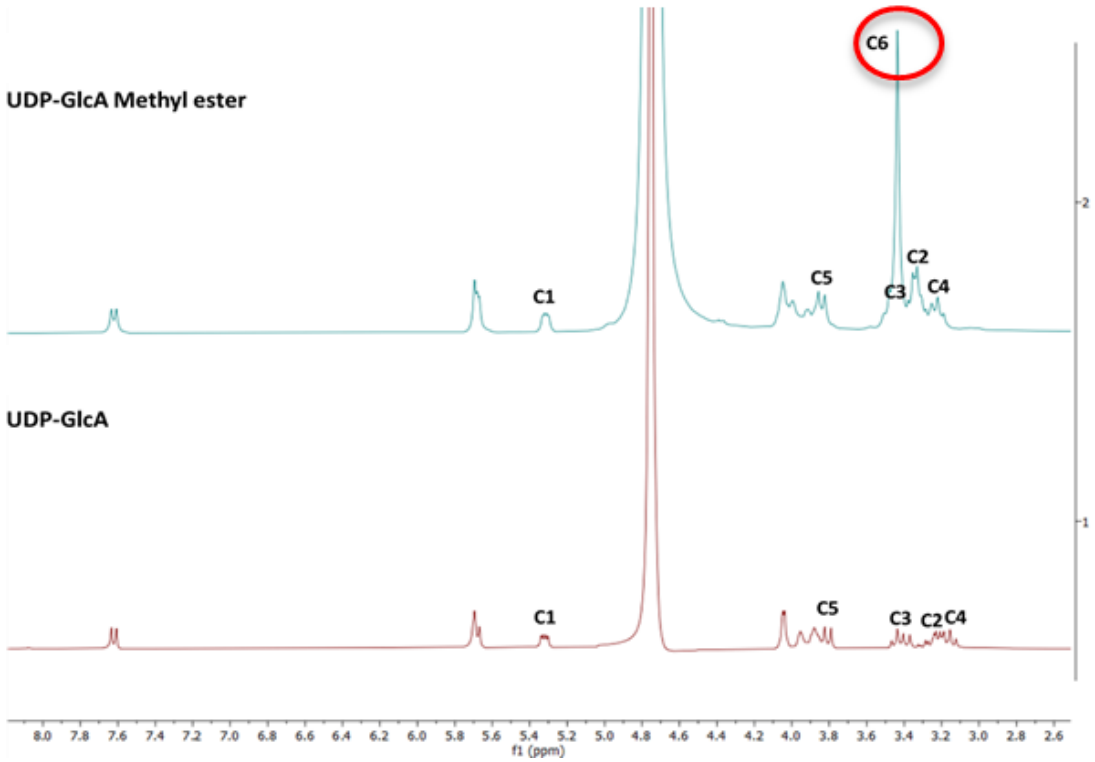

Figure 15. ^{1}H-NMR spectrum of UDP-GlcA methyl ester and UDP-GlcA. The signal coming from methyl group on C6 is labeled with red circle. The signals coming from the protons attached to C1-C5 carbons of UDP-GlcA and UDP-GlcA methyl ester are also shown.

^{1}H-NMR was the final confirmation that the synthesis and isolation of UDP-GlcA methyl ester were succesful with a good purity of obtained compound. This modified ethanol precipitation method seems to be superior compared to the standard DSP, at least for UDP-sugars containing ester bonds. Now, when the unnatural substrate (UDP-GlcA methyl ester) was obtained, activity of the three enzymes towards this substrate was defined (see below).

4.2 PREPARATION OF UXS, UAXS AND UGAepi AND THEIR ACTIVITY TOWARDS UDP-GlcA AND UDP-GlcA methyl ester

Preparation of UXS, UAXS and UGAepi

(1) Gene expression

UXS and UAXS were succesfully expressed in *E. coli* BL21 (DE3) LEMO 21 expression strain [see chapter3.2.2; *(1)*] and purified by His-tag affinity chromatography [see chapter 3.2.2; *(2)*]. UGAepi was already available as purified enzyme (Institute of Biotechnology and Biochemical Engineering, TU Graz). An example of the purification chromatogram from His-tag purification of UAXS is shown in Figure 16.

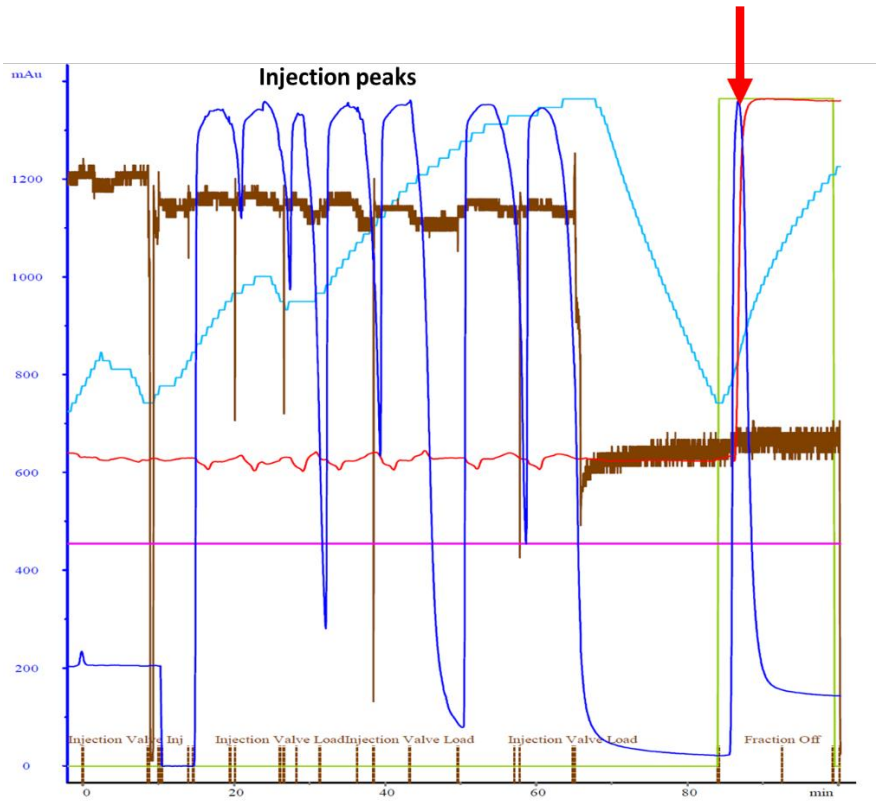

Figure 16. His-tag purification chromatogram of the purification of UAXS. The red arrow shows the elution peak (UAXS). The blue line is UV-absorbance at 280 nm, the brown line stands for pressure, the red line stands for conductivity, the light blue line stands for temperature, the pink line for pH and the green line for concentration. Injection peaks are also shown. Every injection peak marks 10 mL of the cell lysate.

(2) Protein purification by affinity chromatography

UXS was purified by using the same procedure and the chromatogram looked almost the same (dana not shown).

The flowthroughs, washing fractions and elution fractions of UXS and UAXS were collected, as described previously, and the purity of the proteins was checked by SDS-PAGE (Figure 17).

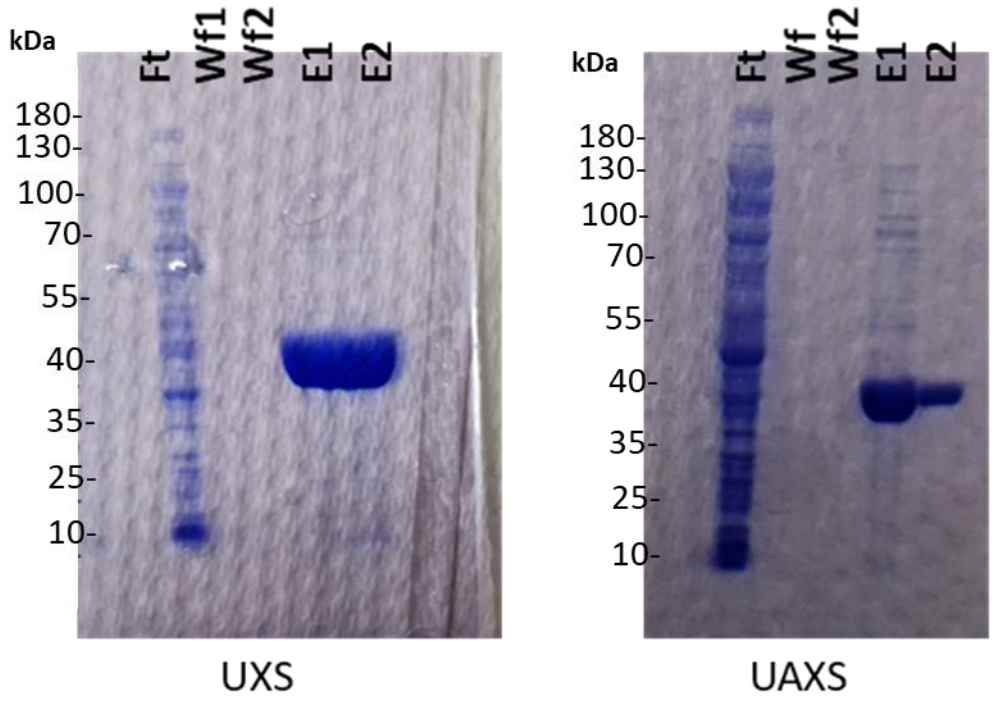

Figure 17. The SDS-PAGE gels of UXS and UAXS. Ft stands for the flowthrough, Wf1 and Wf2 for washing fractions and E1 and E2 for the elution fractions.

The enzymes were obtained in a high purity and a good yield (11 mg per liter of cell culture for UAXS and 34.8 mg per liter of cell culture for UXS) and with their corresponding molecular masses about 38 kDa.

Defining activity of UXS, UAXS and UGAepi towards UDP-GlcA and newly synthesized UDP-GlcA methyl ester was the further step. The aim of those experiments was to compare the enzymatic activity with their natural substrate and the substrate analogue in order to have a better look into the decarboxlyation mechanisms (UXS and UAXS) and the rotation mechanism of UGAepi.

(3) Kinetic studies on UAXS, UXS and UGAepi with two substrates - UDP-GlcA and UDP-GlcA methyl ester

Activity of UXS was tested first with 1 mg/ml of UXS, 0.1 mM of NAD^+ and 2 mg/mL of the substrate (UDP-GlcA or UDP-GlcA methyl ester) at room temperature [see chapter 3.2.2; *(3)*]. Samples from the reaction mixture were taken at the defined time points and analyzed by the HPLC method [see chapter 3.2.1; *(2)*]). Results are shown in Figure 18.

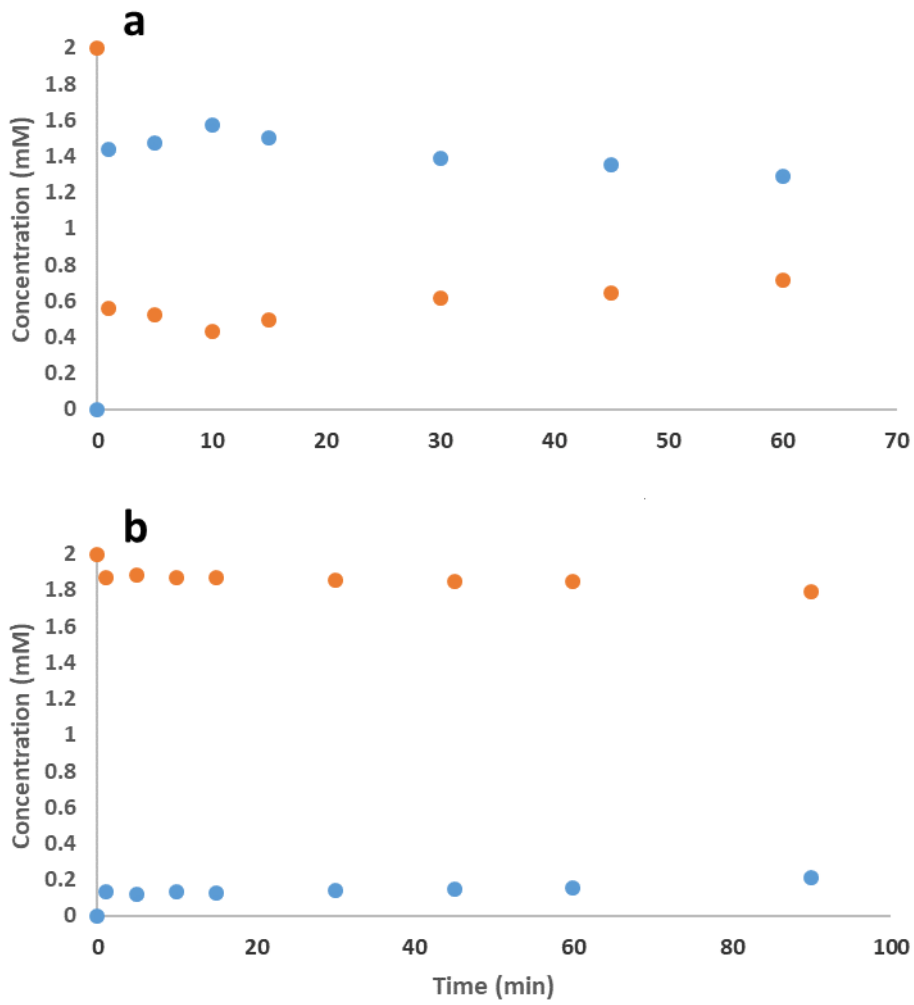

Figure 18. The time courses of UXS (1.0 mg/mL) reaction with UDP-GlcA (a) and UDP-GlcA methyl ester (b). UDP-GlcA and UDP-GlcA methyl ester are shown in orange, the product of enzymatic reaction (UDP-Xyl) is shown in blue.

The specific activity of the enzyme towards UDP-GlcA was 1.4 U/mg (0-1 min). For the reaction with UDP-GlcA methyl ester the specific activity of UXS was 0.13 U/mg (0-1 min).

The 10-fold higher activity of the enzyme towards the natural substrate (UDP-GlcA) than towards substrate analogue (UDP-GlcA methyl ester) was expected. Interestingly, the biphasic behaviour of the enzymatically catalyzed reaction was observed. The inital rate of the reactions was high (0-1 min) and then the reactions seemed to slow down. That strange behaviour was observed with both substrates. In order to exclude that the initial burst of the reaction was dependent on too high enzyme concentration, the reactions were repeated with significantly lower enzyme concentration of 0.3 mg/mL (Figure 19).

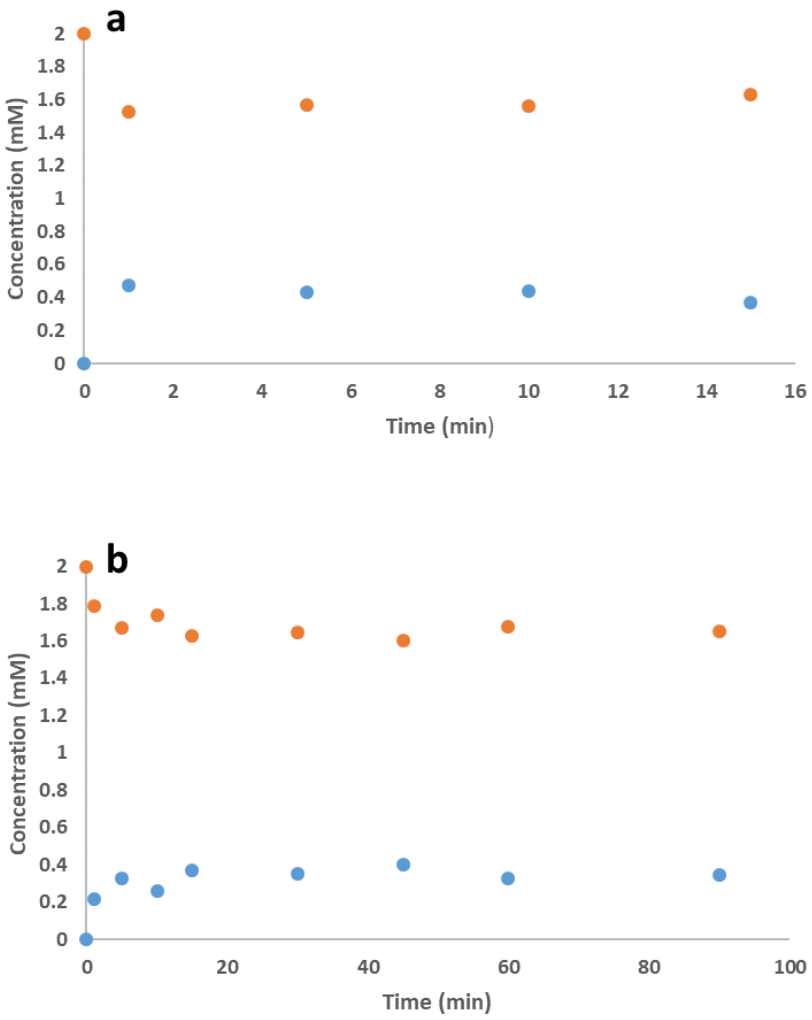

Figure 19. The time courses of UXS (0.3 mg/mL) reaction with UDP-GlcA (a) and UDP-GlcA methyl ester (b). UDP-GlcA and UDP-GlcA methyl ester are shown in orange, UDP-Xyl is shown in blue.

Now, the specific activities were 1.6 U/mg (UXS reaction with UDP-GlcA) and 0.71 U/mg (UXS reaction with UDP-GlcA methyl ester). UXS displayed the same biphasic character again. All of the reactions were performed in the presence of 0.1 mM NAD^+. To explain the strange behaviour, the reactions were repeated with 0.5 mM NAD^+, but the outcome was the same (dana not shown). It seems that the enzyme did not have a problem with the coenzyme. The last experiment was characterization of native UXS by SEC [see chapter 3.2.2; *(2)*] to check the oligomeric state of the native UXS considering that only dimer is an active conformation (Figure 20).

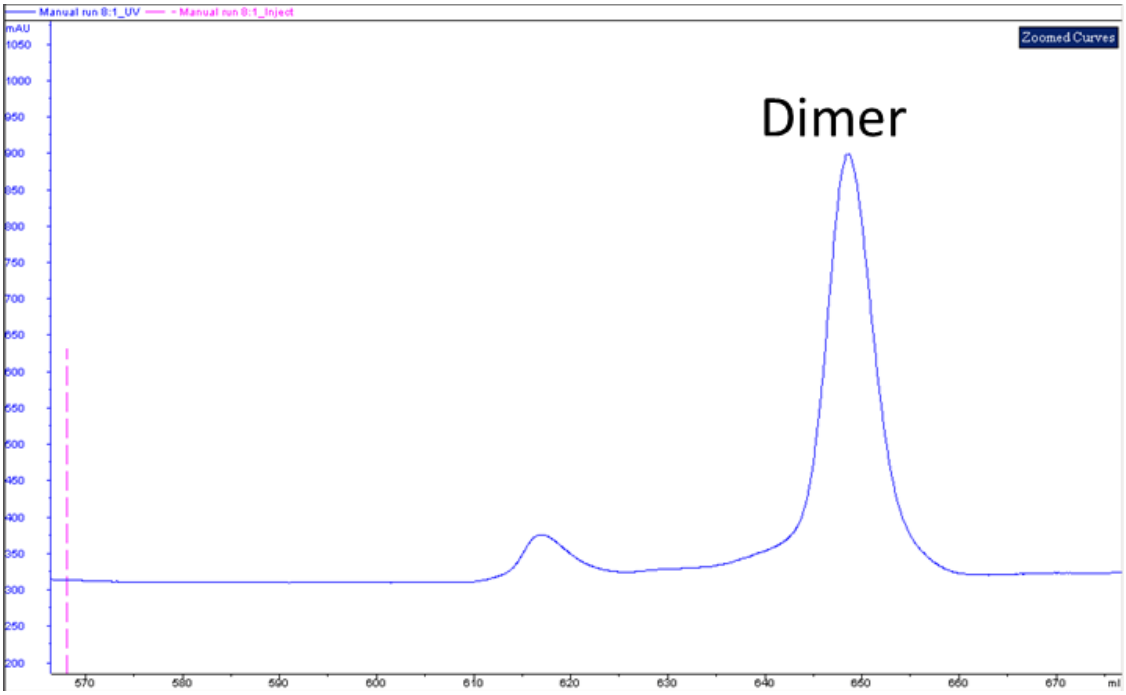

Figure 20. The size-exclusion chromatogram of UXS showing that UXS is in dimeric form.

The chromatogram clearly shows that native UXS with defined specific activity towards the natural and unnatural substrate is mainly present in its dimeric form (>90%). One possible explanation for the biphasic reaction character could be that the product is somehow stuck in the active site preventing the reaction to proceed. Further research is needed to explain that behaviour of the dimeric enzyme. At the moment, it is not possible to interpret it properly.

UAXS was tested almost in the same way like the UXS. Exception was different UAXS concentration use din the activity experiments (2 mg/mL). The outcome of the UAXS catalyzed reaction with UDP-GlcA was expected: the ratio of obtained products (UDP-Xyl and UDP-

Api) was close to 1:1, and completely in a correlation with previous studies (Savino et al., 2019). In addition, a low concentration of the intermediate, UDP-4-keto-pentose is observed (see Figure 22). The specific activity of UAXS towards UDP-GlcA was 0.15 U/mg which is very low (compared to reported 63 mU/mg by (Savino et al., 2019)), possibly because of the loss of activity during the purification and storing of the enzyme. The reaction with UDP-GlcA methyl ester followed the same kinetics, but with 5-fold lower specific activity of only 0.03 U/mg (Figure 21).

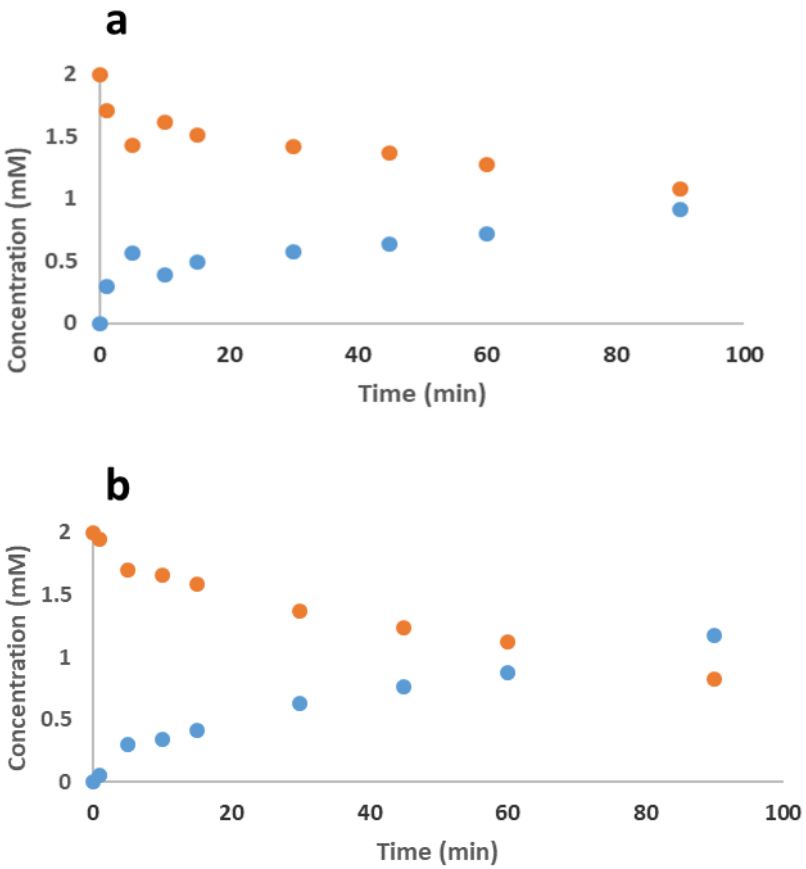

Figure 21. The time courses of UAXS (2 mg/mL) reaction with UDP-GlcA (a) and UDP-GlcA methyl ester (b). UDP-GlcA and UDP-GlcA methyl ester are shown in orange; UDP-Api, UDP-4-keto-pentose and UDP-Xyl are shown in blue.

It was clear that both, UXS and UAXS, accept the substrate analogue as their natural substrate and are able to perform the reaction. The time course analysis was made by using the data from HPLC chromatograms of analyzed samples [see chapter 3.2.1; *(2)*]). At first, each sample was run for only 5 min and it was not possible to have a good separation between the products peaks (UDP-Api, UDP-Xyl and UDP-4-keto-pentose). Therefore another protocol [the HPLC

method, see chapter 3.2.2; *(3)*] was used. The peaks from UDP-Api and UDP-Xyl corresponded to the previously published data for the UXS and UAXS reactions with UDP-GlcA (Savino et al., 2019). It was the confirmation that both enzymes are able to produce the same products from either UDP-GlcA or UDP-GlcA methyl ester (Figure 22).

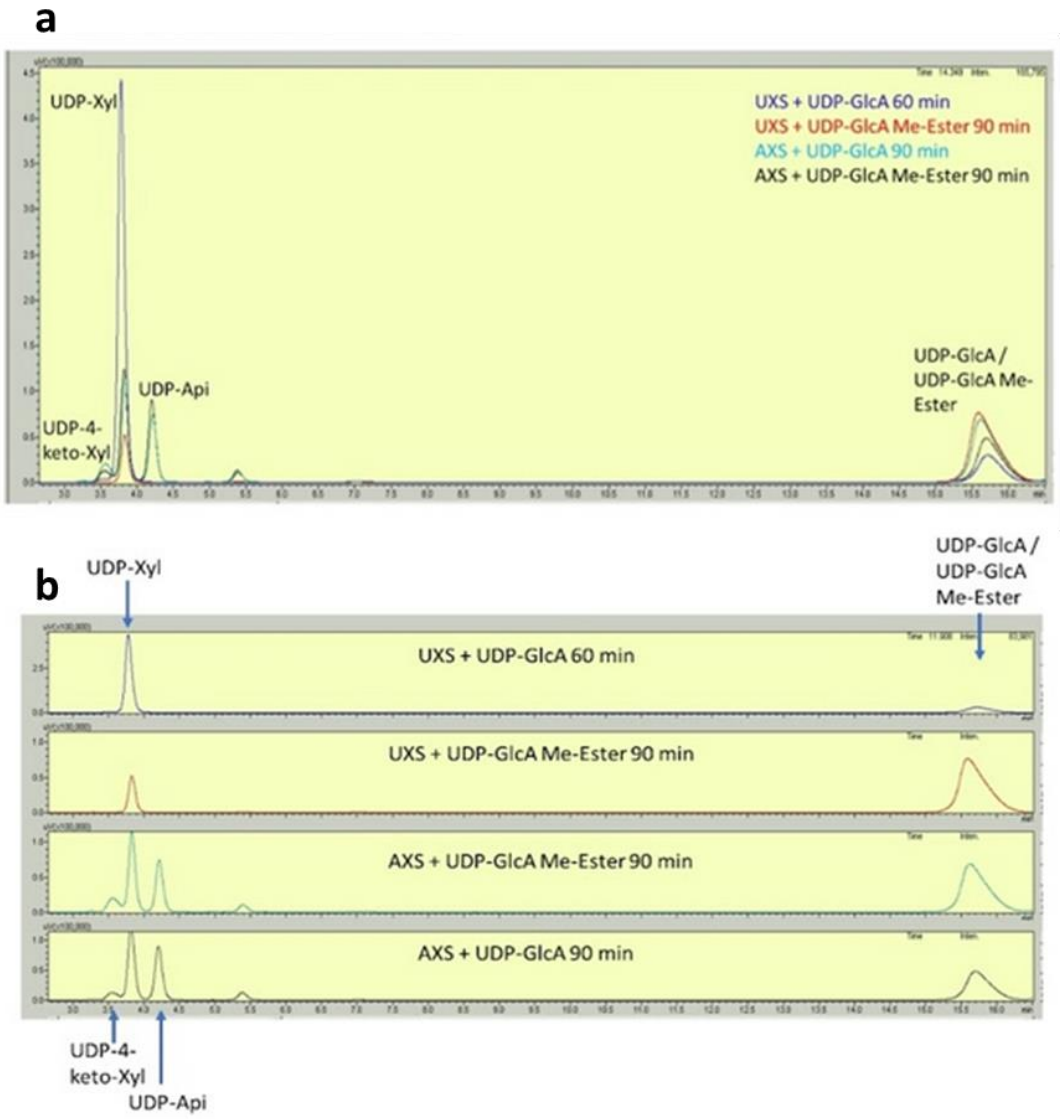

Figure 22. The product pattern of UXS and UAXS reactions (60 and 90 min time points) with UDP-GlcA and UDP-GlcA methyl ester obtained by the HPLC method [see chapter 3.2.2; *(3)*]: (a) the overlay of the chromatograms and (b) separated chromatograms. The products and the substrates are marked with blue arrows. UDP-4-keto-pentose is labeled as UDP-4-keto-Xyl.

As shown in Figure 22, the enzymes (UXS and UAXS) are able to produce the same products (UDP-Xyl, UDP-Api and UDP-4-keto-pentose) from both substrates (UDP-GlcA and UDP-GlcA methyl ester) by hydrolyzing the ester bond of UDP-GlcA methyl ester which was confirmed by ^{1}H-NMR analysis of the UXS, UAXS and UGAepi reactions with UDP-GlcA

methyl ester in D_2O (see chapter 3.2.2; *Identification of products-UDP-Api, UDP-Xyl and UDP-GalA by ^{1}H-NMR*, Figure 23).

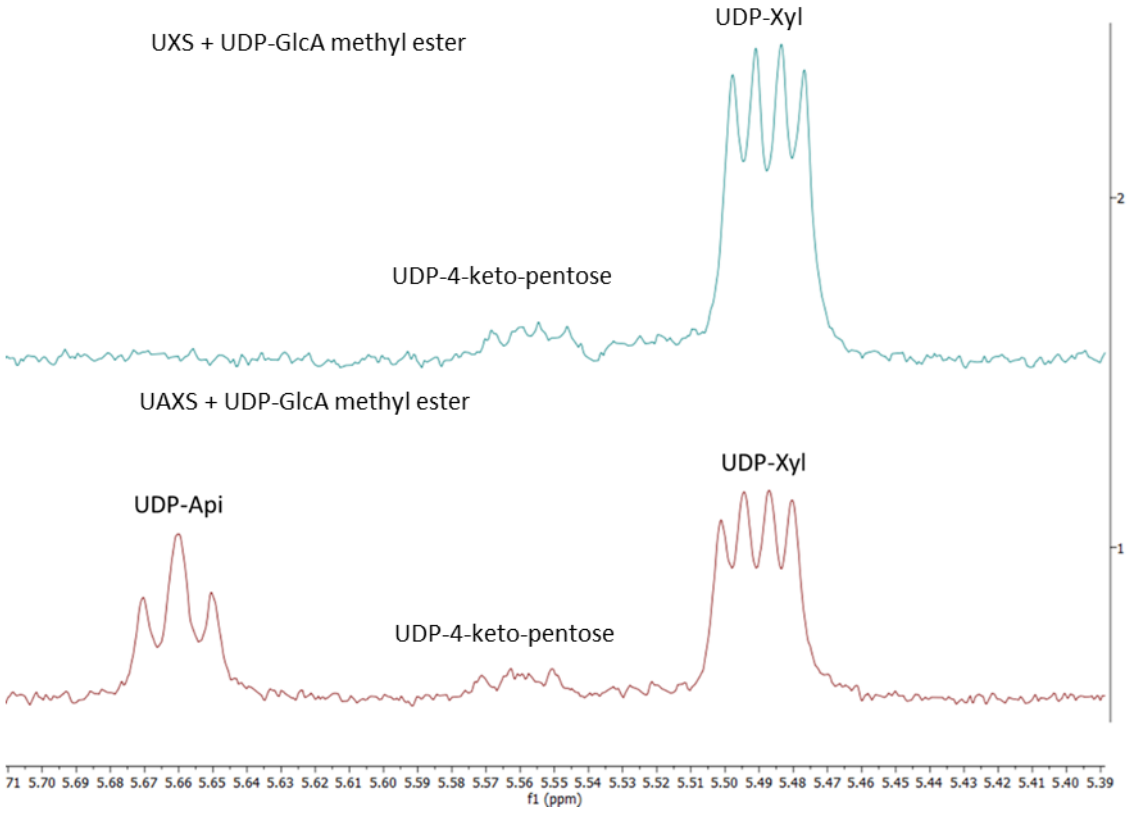

Figure 23. A close-up of anomeric regions in ^{1}H-NMR spectrum of end-points (90 min) of UXS (blue) and UAXS (red) reactions with UDP-GlcA methyl ester. The signals coming from UDP-Api, UDP-Xyl and UDP-4-keto-pentose formed in the reactions are highlighted.

Alongside the complexity of their mechanisms, these enzymes are even able to somehow incorporate the hydrolysis into their activity in order to perform the decarboxylation of UDP-GlcA methyl ester and produce UDP-Xyl, UDP-Api and UDP-4-keto-pentose.
Then, activity of UGAepi was tested firstly by adding 0.07 mg/mL of the enzyme, but it was too high concentration since the enzyme was too fast and it was not possible to have a trackable kinetics. The enzyme activity was then tested with with its concentration of 0.035 mg/mL towards both substrates (UDP-GlcA and UDP-GlcA methyl ester; Figure 24).

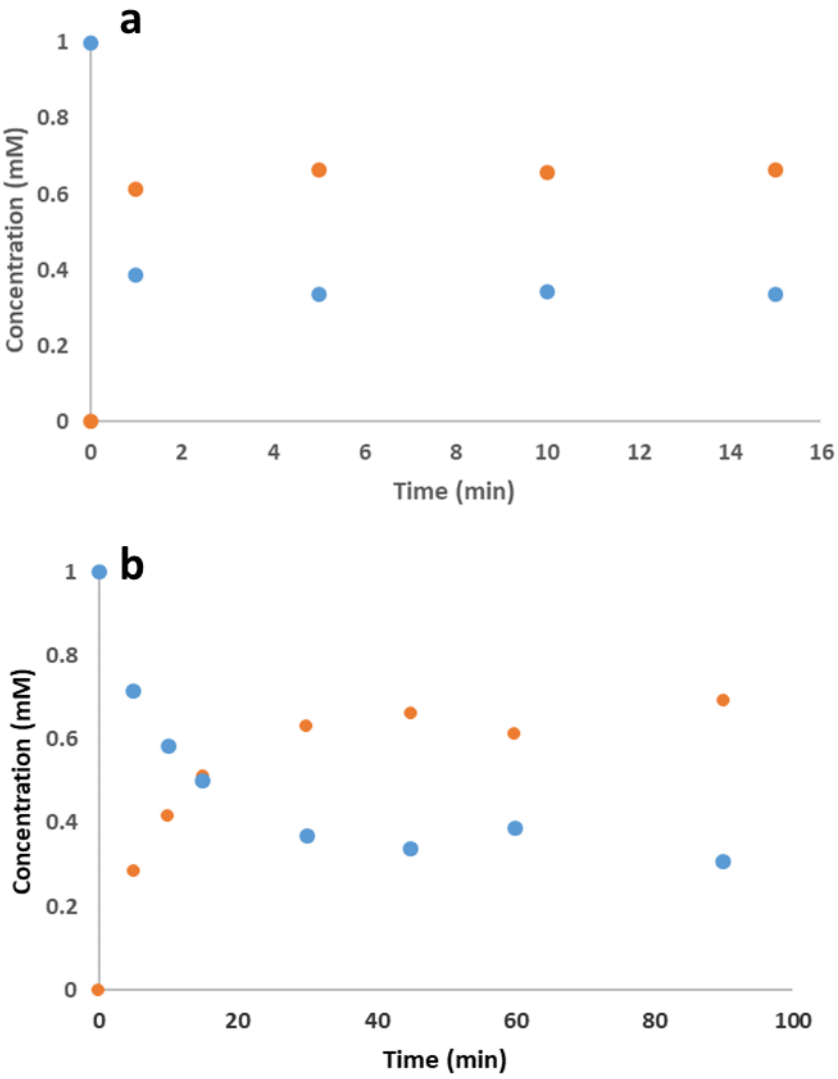

Figure 24. The time courses of UGAepi (0.035 mg/mL) reactions with UDP-GlcA (a) and UDP-GlcA methyl ester (b). UDP-GalA is shown in orange, UDP-GlcA (a) and UDP-GlcA methyl ester (b) are shown in blue.

The specific activity of UGAepi in the reaction with UDP-GlcA was 0.53 U/mg while the specific activity of the enzyme in the reaction with UDP-GlcA methyl ester was 0.65 U/mg. The role of Arg185 residue in the active site of the enzyme is well known - it stabilizes UDP-GalA and prevents the decarboxylation of UDP-GlcA. In case of UDP-GlcA methyl ester, due to the ester moiety instead of a carboxylate, the salt bridge cannot be established between UDP-GlcA methyl ester and Arg185. In fact, the specific activity of the enzyme reaction with UDP-GlcA methyl ester is slightly higher than the specific activity with UDP-GlcA. One explanation could be that fewer ionic interactions allow UGAepi to perform the rotation faster and still

stabilize the product (UDP-GalA). Figure 25 shows the HPLC chromatograms of UGAepi reactions.

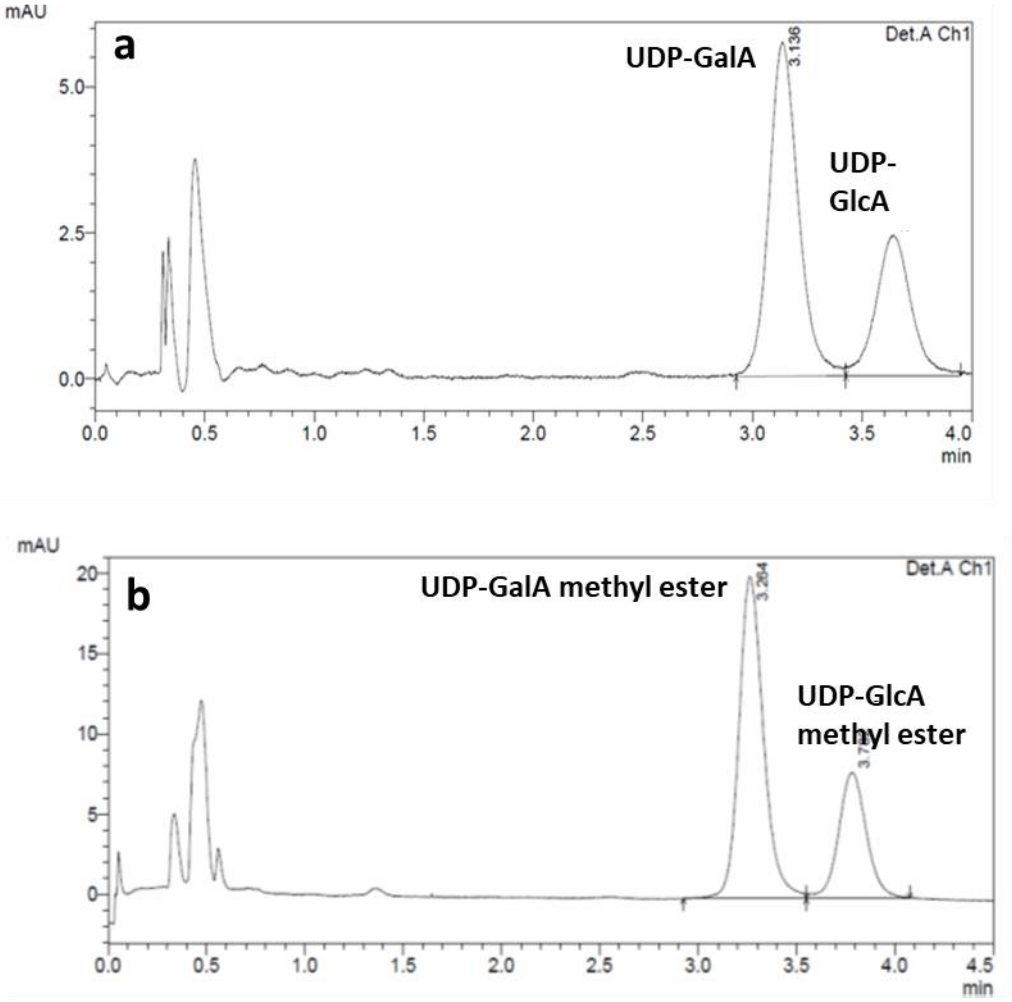

Figure 25. The HPLC chromatograms showing the end points (90 min) of UGAepi (0.035 mg/mL) reactions with UDP-GlcA (a) and UDP-GlcA methyl ester (b) analyzed by the HPLC method [see chapter 3.2.2; *(3)*].

The peaks from UDP-GlcA/UDP-GalA (Figure 25, a) and the peaks from UDP-GlcA methyl ester/UDP-GalA methyl ester could not have been separated by the HPLC method [see chapter 3.2.2; *(3)*], therefore the UGAepi reaction with UDP-GlcA methyl ester was run in D_2O and the end-point was analyzed by ^{1}H-NMR to confirm the products identities (Figure 26).

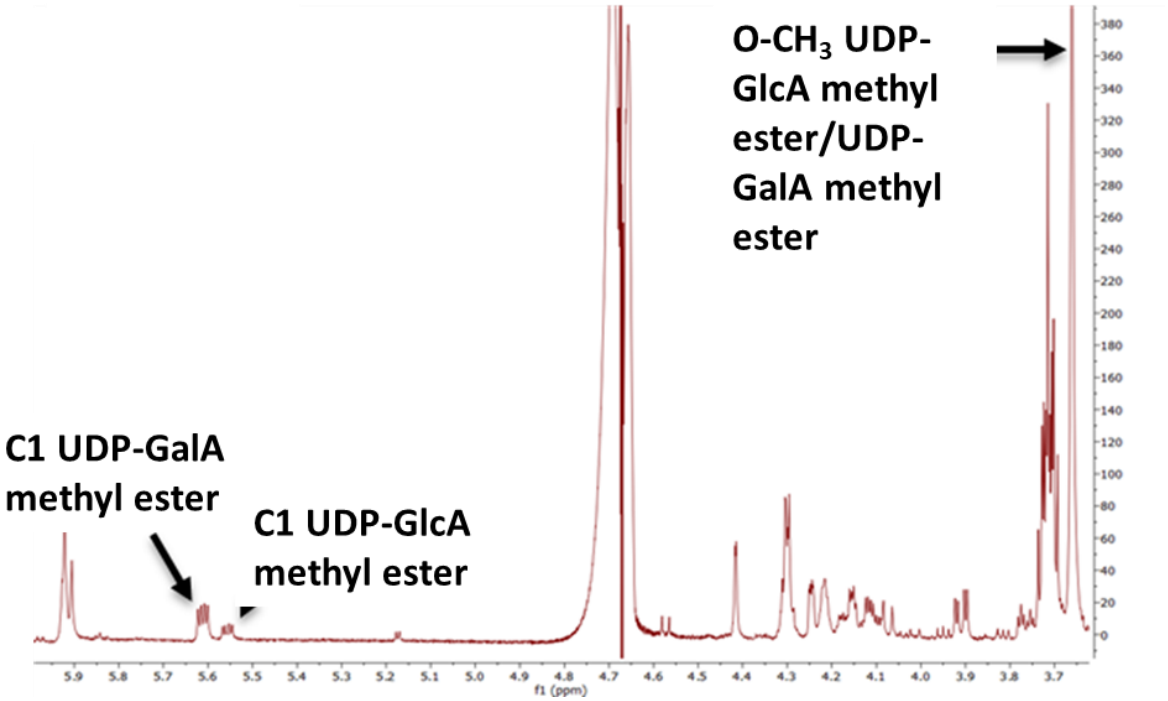

Figure 26. ^{1}H-NMR spectrum of the end-point (90 min) of the UGAepi reaction with UDP-GlcA methyl ester showing the signals coming from methyl/methanol. The signals coming from the anomeric C1 atoms of UDP- GlcA methyl ester and UDP-GalA methyl ester are also shown.

The spectrum obtained from the reaction indicates that the signal on C6 comes from a methyl group. However, that signal also appears in NMR spectra from UXS and UAXS (Figure 27) meaning that it is not possible to distinguish whether the signals come from methanol or methyl group. For the further analysis, in order to determine the origin of the signal, establishing the methanol quantification method was necessary.

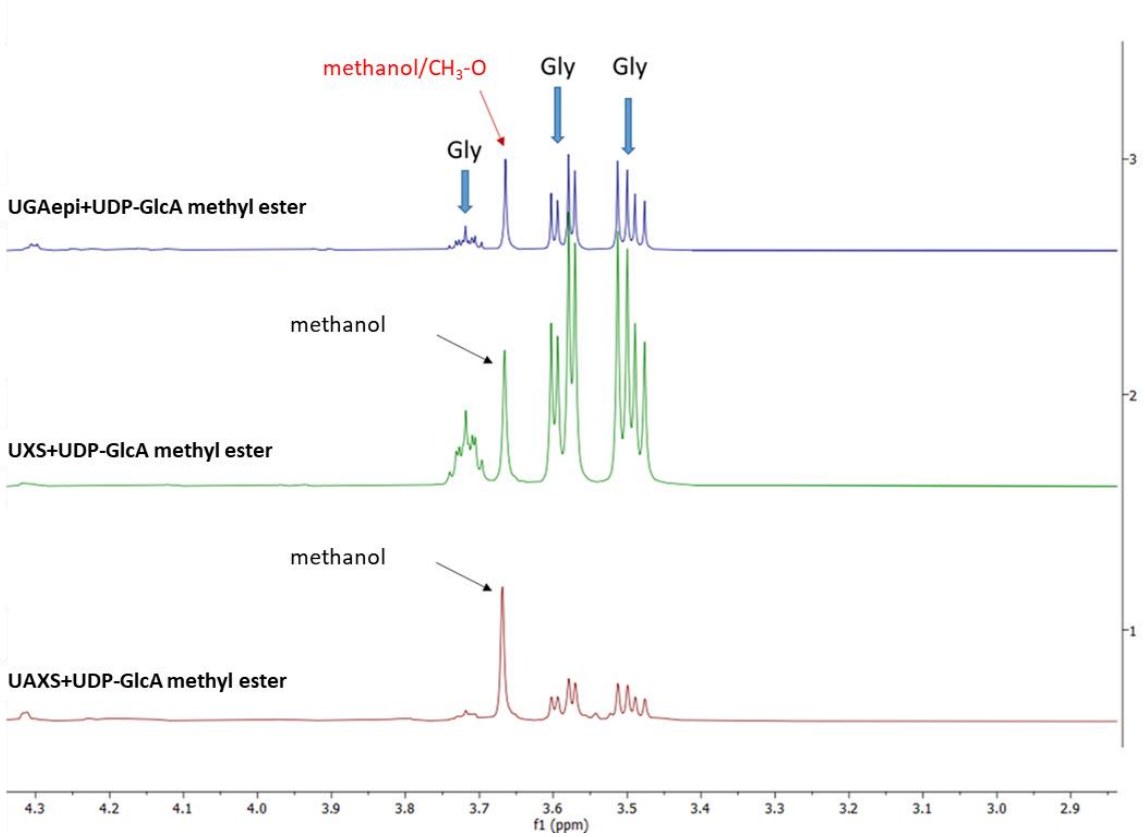

Figure 27. A comparison of ^{1}H-NMR spectra obtained from the reactions of UGAepi (blue), UXS (green) and UAXS (red) with UDP-GlcA methyl ester. The signal coming from methanol/CH_3-O is shown. Gly stands for glycerol residual from the storage buffer of UGAepi.

Monitoring the methanol formation during UDP-GlcA methyl ester conversion by UXS, UAXS and UGAepi

The methanol quantification method was based on measuring the concentration of NADH released from formaldehyde dehydrogenase and alcohol oxidase reactions (see chapter 3.2.2; *Monitoring the methanol formation during UDP-GlcA methyl ester conversion by UXS, UAXS and UGAepi*; (Vlnet, 1987). Assuming that UXS, UAXS initiate the methanol release in their reactions and UGAepi does not, the absorbance at 340 nm should be increasing for UXS and UAXS reactions until these reactions stop. As previously described, 1 mol of released NADH corresponds to 1 mol of formed methanol (see chapter 3.2.2; *Monitoring the methanol formation during UDP-GlcA methyl ester conversion by UXS, UAXS and UGAepi*). The concentration of expected methanol release was supposed to be in the middle of the concentration range of the calibration curve. The calibration curve was prepared by taking the end points (40 min) of the reactions with 0, 0.1 and 0.3 mM of methanol (Figure 28).

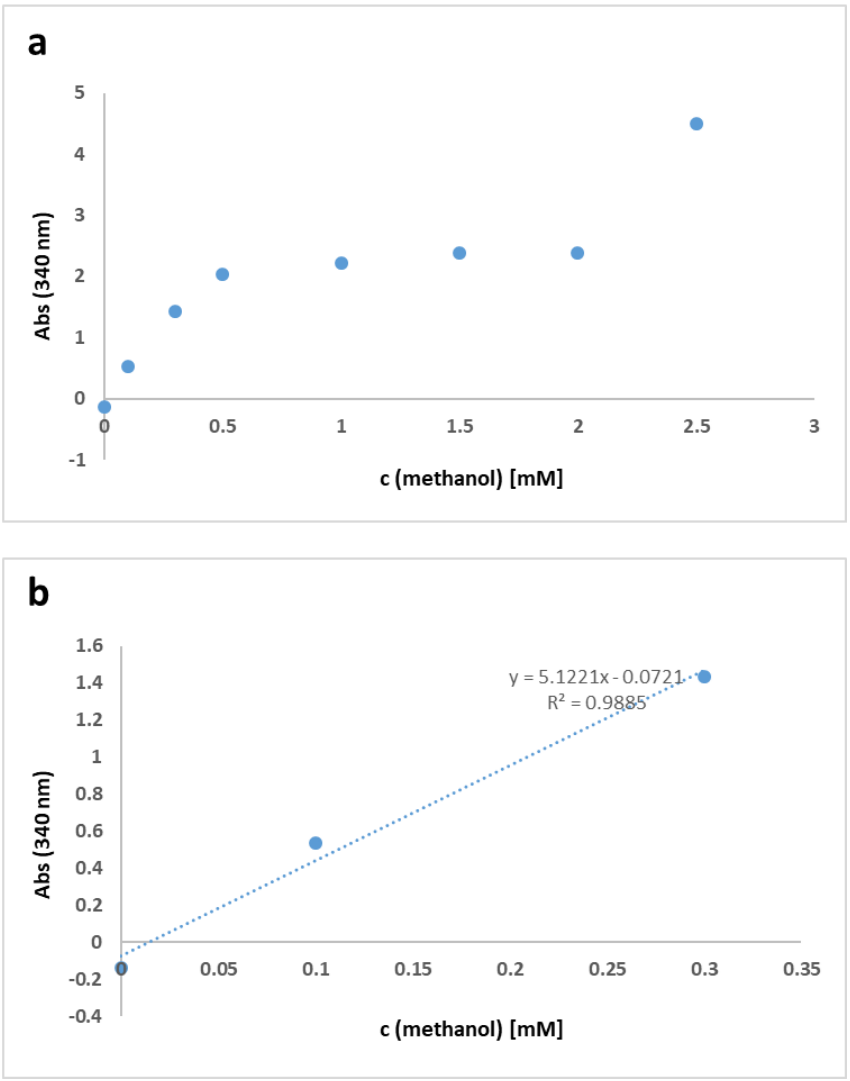

Figure 28. Methanol calibration curve - (a) all the methanol concentrations included. (b) the calibration curve with the first three points.

Only the first three points (0, 0.1 and 0.3 mM of methanol) were taken to prepare the calibration curve because correlation between methanol concentration and absorbance at wavelength of 340 nm is linear until absorbance reaches 1.8 AU. The values were also checked by Lambert-Beer's law to confirm the accuracy of the calibration curve.

Before starting the reactions with UDP-GlcA and UDP-GlcA methyl ester with enzymes (UXS, UAXS and UGAepi), the methanol contamination or unspecific oxidation of the substrates was checked. The reactions were done by adding either UDP-GlcA methyl ester or UDP-GlcA together with enzymic reagent and alcohol oxidase, while UGAepi, UXS and UAXS were not added to the mixture (see chapter 3.2.2; *Monitoring the methanol formation during UDP-GlcA methyl ester conversion by UXS, UAXS and UGAepi*). The reaction containing UDP-GlcA

methyl ester was spiked with 0.3 mM methanol to confirm the reliability of the assay (Figure 29).

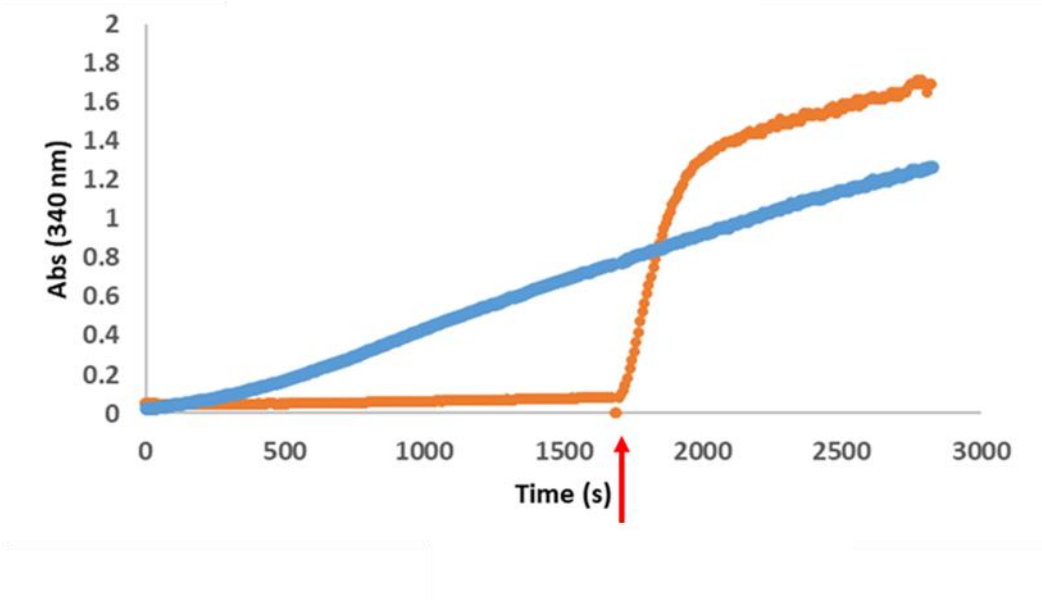

Figure 29. Increase of absorbance (340 nm) of the reaction mixture containing UDP-GlcA methyl ester (orange) and UDP-GlcA (blue) with formaldehyde dehydrogenase and alcohol oxidase. Red arrow indicates the time point when UDP-GlcA methyl ester reaction was spiked with 0.3 mM of methanol.

As expected, in reaction with UDP-GlcA methyl ester methanol was not released, only added 0.3 mM of methanol was observed implying that the substrate did not have any methanol contamination. Based on the calibration curve (Figure 28b), the methanol concentration in the end-point of the reaction was 0.37 mM which was acceptable since the absorbance of 1.8 AU slightly exceeds the linear range. On the other hand, there was a problem with UDP-GlcA. It was observed that the methanol concentration was increasing constantly in the reaction mixture with this natural substrate. The problem could be that the compund had a residual impurity originated from the purification after synthesis. Better explanation might be obtained after additional experiments.

UXS, UAXS and UGAepi were tested with 1.6 mM of UDP-GlcA methyl ester and the reactions were running for 40 min. All of the reactions were also analyzed by the HPLC method [see chapter 3.2.2; *(3)*] and the concentrations of the released methanol were calculated using the calibration curve (Figure 28b). The data obtained by spectrophotometric measuremets of NADH and by the HPLC method [see chapter 3.2.2; *(3)*] are shown in Figure 30.

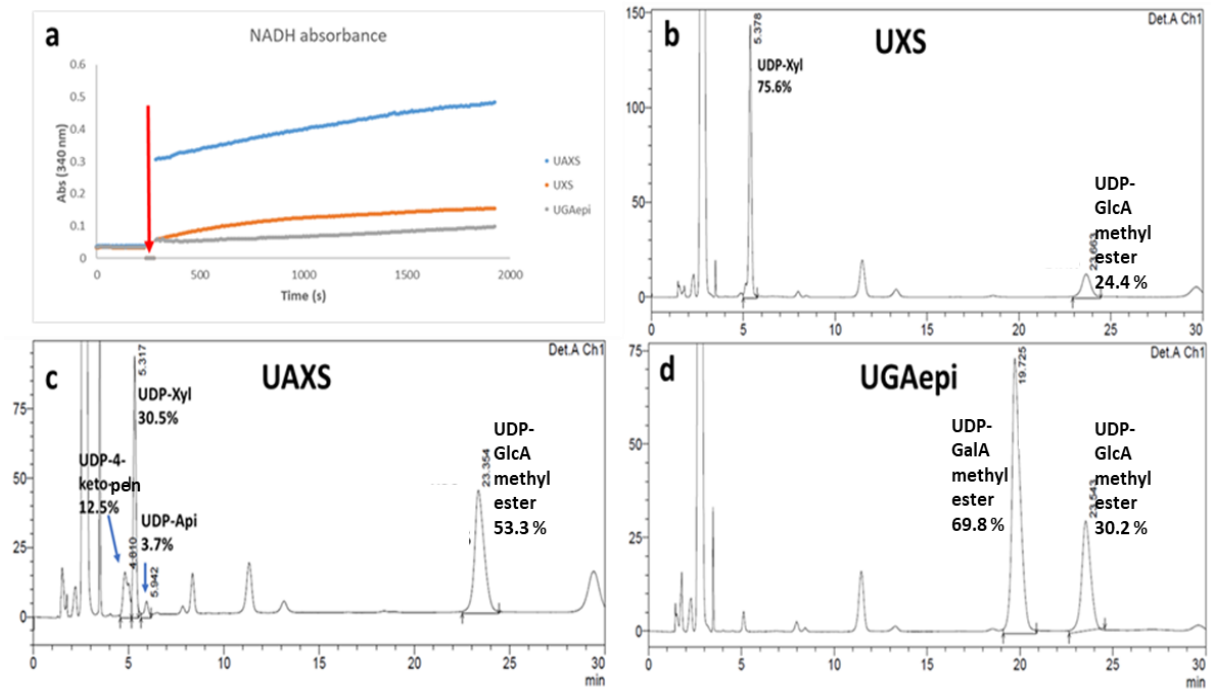

Figure 30. The spectrophotometric (a) and HPLC data (b, c, d) of UXS reaction with UDP-GlcA methyl ester (b); UAXS reaction with UDP-GlcA methyl ester (c); and UGAepi reaction with UDP-GlcA methyl ester (d). The figure 30. (a) showing the methanol concentration increase after the addition of UXS (0.3 mg/mL), UAXS (2 mg/mL) and UGAepi (0.035 mg/mL) to the enzymic reagent and UDP-GlcA methyl ester mixture (see chapter 3.2.2; *Monitoring the methanol formation during UDP-GlcA methyl ester conversion by UXS, UAXS and UGAepi*). The red arrow points the time point when the enzymes were added to that mixture. (b) HPLC chromatogram of UXS reaction with UDP-GlcA methyl ester after 40 min [see chapter 3.2.2; *(3)*]. (c) HPLC chromatogram of UAXS reaction with UDP-GlcA methyl ester after 40 min [see chapter 3.2.2; *(3)*]. UDP-4-keto-pen stands for UDP-4-keto-pentose. (d) HPLC chromatogram of UGAepi reaction with UDP-GlcA methyl ester after 40 min [see chapter 3.2.2; *(3)*].

The concentration of formed product (UDP-Xyl) in UXS reaction was 1.2 mM, but the calculated methanol concentration was 52-fold lower. UAXS produced 0.75 mM of decarboxylated products (UDP-Api and UDP-Xyl), 9-fold higher than the released methanol concentration. UGAepi produced 1.12 mM of product (UDP-GalA methyl ester) which was 224-fold more than the methanol concentration calculated from the calibration curve (0.005 mM). The results obtained with UGAepi could support the assumption that the enzyme does not hydrolyze the ester bond in UDP-GlcA methyl ester and does not initiate methanol release. To explain the case of UXS, it has to be considered that optimal pH for UXS activity is 8.0.

The reaction (see chapter 3.2.2; *Monitoring the methanol formation during UDP-GlcA methyl ester conversion by UXS, UAXS and UGAepi*) was carried out at pH 7.6 in 0.1 M Na_2HPO_4/KH_2PO_4 phosphate buffer containing Na^+ ions which are usual conditions for the epimerase. UAXS performs significantly better than UXS, but the enzyme was added in a higher concentration (2 mg/mL) than UXS (0.3 mg/mL). Furthermore, pH of 7.0 is usually optimal for UAXS reaction. The reaction conditions (see chapter 3.2.2; *Monitoring the methanol formation during UDP-GlcA methyl ester conversion by UXS, UAXS and UGAepi*) were the most suitable for UGAepi and the result was the closest to what was assumed. It should be mentioned, based on previous kinetic experiments, that UXS and UAXS had a different behaviour with the same substrate. Those evidences might be supporting that UXS and UAXS hydrolyze the ester while UGAepi does not. However, to confirm that fact, the methanol assays should be optimized specifically for each enzyme. First of all, pH for UXS and UAXS could be adjusted to either 8.0 (UXS) or 7.0 (UAXS) in order to ensure that the enzymes work in optimal conditions. Secondly, UXS may be added in a higher concentration to have a better comparison with UAXS. Lastly, since NAD^+ concentration in the enzymic reagent (see chapter 3.2.2; *Monitoring the methanol formation during UDP-GlcA methyl ester conversion by UXS, UAXS and UGAepi*) is relatively high (2.5 mM), it could be that it is reduced by formaldehyde dehydrogenase which causes the apparent NADH increase in UGAepi (0.035 mg/mL) reaction.

4.3 PRODUCTION OF A NOVEL BACTERIAL UDP-APIOSE/XYLOSE SYNTHASE (GrUAXS) AND ITS MUTANT

(1) Transformation of pET28a_GrUAXS into E. coli BL21 (DE3) LEMO21 cells

GrUAXS is interesitng for the reaserch because of its difference in the active site residues compared to UAXS wild-type from *Arabidopsis thaliana*. In a position 120 GrUAXS has serine instead of cysteine (position 140 in UAXS wild-type; (Smith and Bar-Peled, 2017). GrUAXS (pET28a_GrUAXS) was expressed in *E. coli* BL21 (DE3) LEMO21 expression strain and purified by His-tag purification (see chapter 3.2.1; *Protein purification by affinity chromatography*).

(2) Gene expression

The first expression trial with standard expression conditions (0.2 mM IPTG, 120 rpm for 18 h at 18 °C, see chapter 3.2.1; *Gene expression, transformed E. coli strains cultivation and cell extract preparation*) was not successful since the enzyme was not expressed. The optimization meant changing the incubation conditions after inducing the expression of the gene by IPTG [see chapter 3.2.3; *(2)*]. The incubation time was shortened to 4 h and the temperature increased to 30 °C according to the previously published data (Smith and Bar-Peled, 2017).

(3) GrUAXS purification by affinity and size-exclusion chromatography

Before harvesting, 1.5 mL of cell culture containing GrUAXS was taken and treated by B-PER™ Bacterial Protein Extraction Reagent to determine the presence of GrUAXS in *E. coli* BL21 (DE3) LEMO21. The samples prepared by this protocol were run on SDS-PAGE (Figure 31). The enzyme was purified by His-tag purification and run through SEC column in order to isolate the active dimer [see chapter 3.2.3; *(3)*] since the enzyme is prone to aggregation (Smith and Bar-Peled, 2017) The protein yield was 7.5 mg/L which was enough for the purpose of this work.

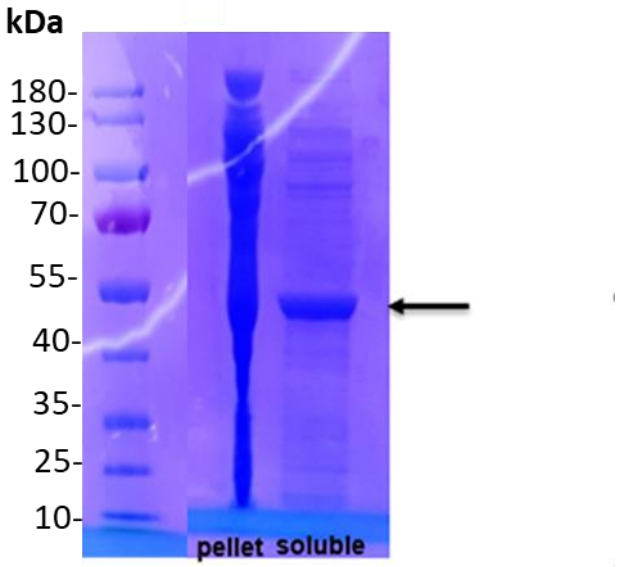

Figure 31. SDS-PAGE of GrUAXS after optimization [see chapter 3.2.3; *(2)*], obtained by B-PER™ Bacterial Protein Extraction Reagent protocol and running the insoluble (pellet) and soluble fractions. GrUAXS is marked with the arrow and shown in soluble fraction with its corresponding molecular mass of about 48 kDa.

(4) Activity of GrUAXS towards UDP-GlcA

The enzyme activity was tested towards UDP-GlcA by using 0.2 mg/mL or 5 mg/mL of the enzyme. The reaction with 0.2 mg/mL did not show any activity because the enzyme concentration was too low. The time course for the reaction with 5 mg/mL of GrUAXS is shown in Figure 32.

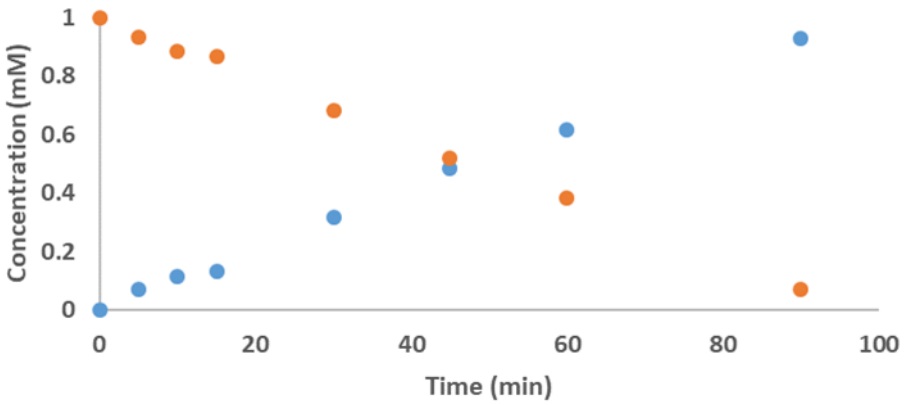

Figure 32. The time course of GrUAXS (5 mg/mL) reaction with UDP-GlcA (orange). UDP-Api, UDP-Xyl and UDP-4-keto-pentose are shown in blue.

The specific activity of GrUAXS (5 mg/mL) was 2.1 mU/mg and k_{cat} of 0.09 min^{-1} (k_{cat}=Vmax/[E]) while corresponding values of 420 mU/mg and k_{cat} of 906 min^{-1} were reported by Smith and Bar-Peled (Smith and Bar-Peled, 2017). The reason for that might be that GrUAXS in this thesis was not the same enzyme as reported by Smith and Bar-Peled (2017). It may have been the mistake made during the sequencing. In a comparison, k_{cat} of UAXS wild-type is 0.49 min^{-1} and UAXS C140S variant has k_{cat} of 0.07 min^{-1} (Savino et al., 2019). UAXS wild-type produces UDP-4-keto-pentose, UDP-Xyl and UDP-Api in a ratio 1 : 1 : 1, while GrUAXS produces UDP-4-keto-pentose : UDP-Xyl : UDP-Api in ratio of 1 : 2 : 2 (Figure 33).

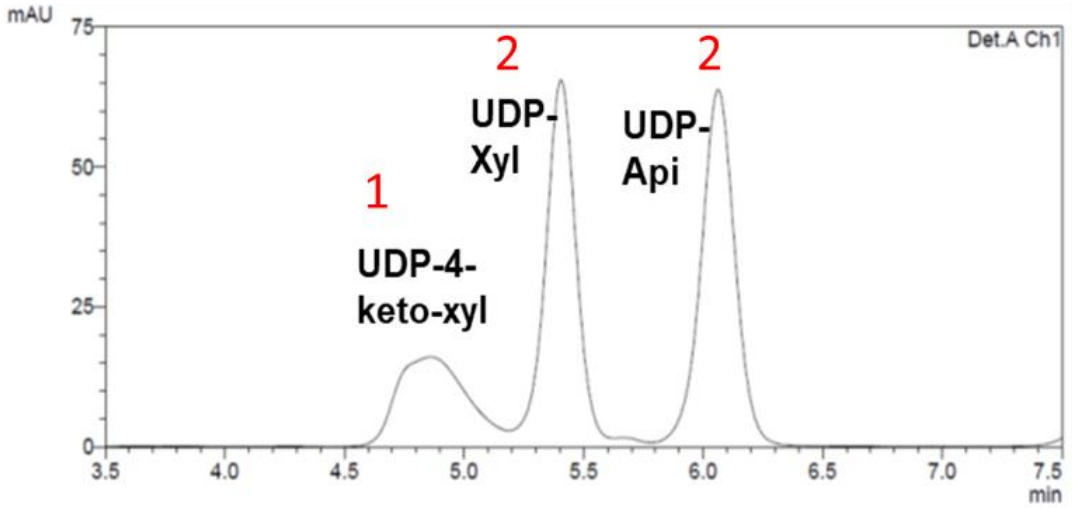

Figure 33. HPLC chromatogram of GrUAXS reaction with UDP-GlcA after 90 min obtained in Kinetex® column (5 µm EVO C18 100 Å, 150 x 4.6 mm) [see chapter 3.2.2; (3)] showing the ratio of formed products UDP-Api : UDP-Xyl : UDP-4-keto-xyl = 1:2:2.

The obtained data suggests that Cys140 (Cys120) could have the same role in both, GrUAXS and UAXS wild-type. Given that the UAXS wild-type has about 6-fold higher k_{cat} value than GrUAXS, for further conclusions the mutagenesis study on GrUAXS was necessary.

(5) Mutagenesis, expression optimization, purification and activity of GrUAXS S120C variant

The aim was to introduce the mutation at position 120 in the active site of GrUAXS in order to create GrUAXS S120C variant and possibly increase the enzyme activity. The mutation was introduced by PCR using pET28a_GrUAXS as a template [see chapter 3.2.3; *(5)*]. The PCR mixture was purified and transformed into *E. coli* NEB5α strain, as described previously [see chapter 3.2.3; *(5)*]. The cells were grown and the plasmid was isolated, sequenced and transformed into *E. coli* BL21 (DE3) LEMO21 expression strain [see chapter 3.2.3; *(1)*]. The expression required the optimizations of the conditions: the incubation temperature, the incubation time, the shaking speed and the IPTG concentration, because it was not possible to express GrUAXS S120C variant under the standard expression conditions used for GrUAXS wild-type. The SDS-PAGE gels displaying the expression progress are shown in Figure 34.

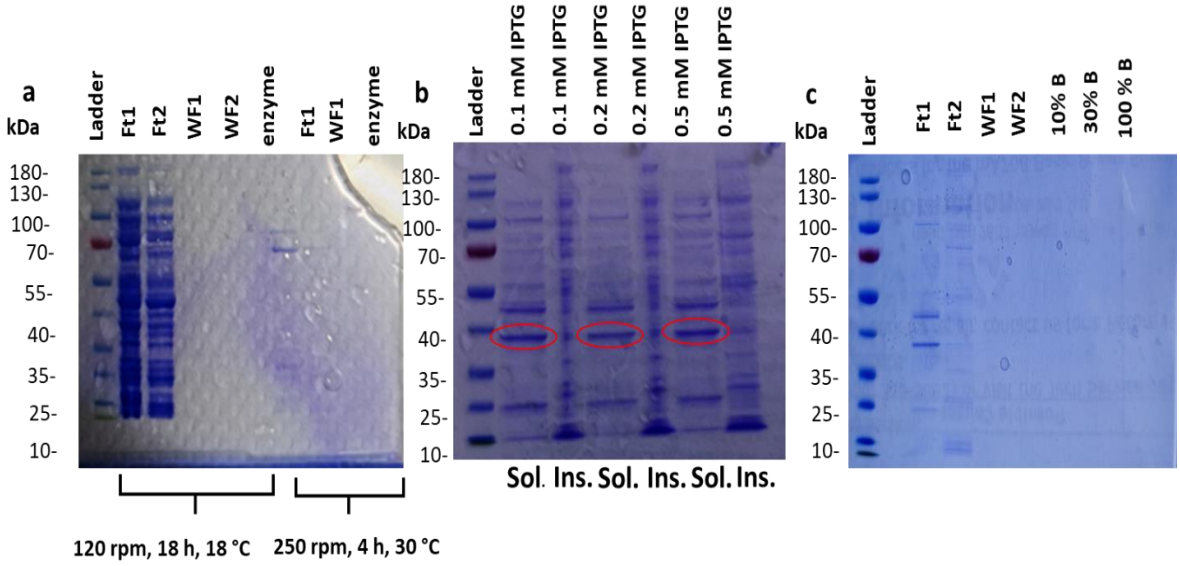

Figure 34. SDS-PAGE gels showing the expression optimization progress for GrUAXS S120C variant. (a) The SDS-PAGE gel of the samples after His-tag purification [see chapter 3.2.3; *(3)*] after two different expression conditions: 120 rpm (18 h, 18 °C) and 250 rpm (4 h, 30 °C). (b) The SDS-PAGE gel of the samples prepared by B-PER™ Bacterial Protein Extraction Reagent treatment [see chapter 3.2.3; *(5)*]. for three different IPTG concentrations (120 rpm, 18 h, 18 °C). Red circles mark the GrUAXS S120C. (c) The SDS-PAGE gel after His-tag purification of GrUAXS S120C obtained from different expression conditions (b)[see chapter 3.2.3; *(5)*]. Sol stands for soluble and Ins for insoluble fractions; 10%, 30%, 100% B stands for the proportion of His-trap elution buffer (B) [see chapter 3.2.3; *(5)*].; Ftn stands for flowthrough, WFn for washing fraction and enzyme for merged and concentrated elution fractions.

Although a couple of different conditions were tried, the enzyme could not be successfully purified. Unlike the wild-type, the GrUAXS S120C mutant does not tolerate harsh expression conditions suggesting that the expressed protein might have a folding problem caused by the mutation. Further optimizations are needed, *e.g.* adding the ethanol or rhamnose before inducing or together with IPTG.

Considering that the experiment with B-PER™ Bacterial Protein Extraction Reagent confirmed the presence of S120C variant, the 100% B fraction was concentrated and the enzyme activity towards UDP-GlcA tested (Figure 35).

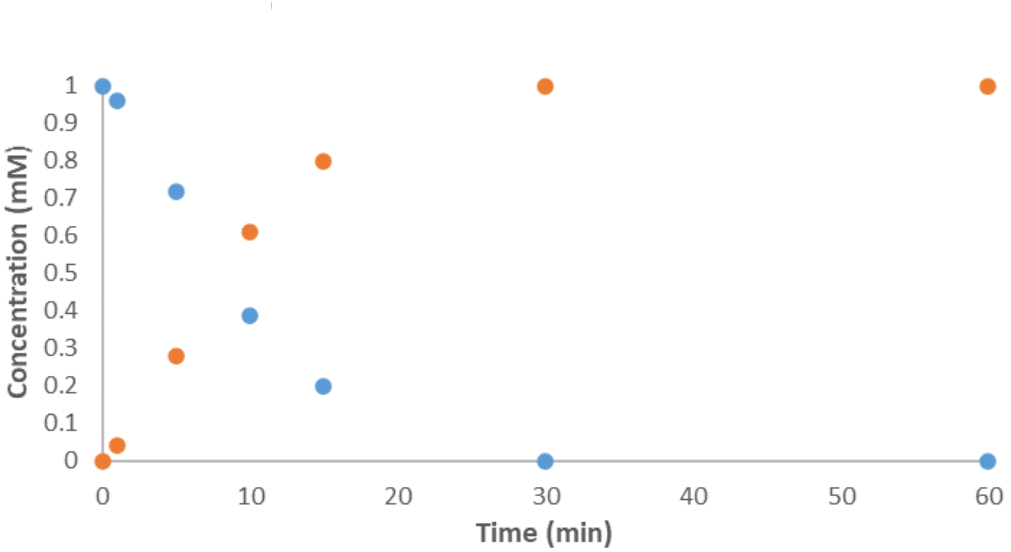

Figure 35. The time course of the GrUAXS S120C (5 mg/ml) reaction with UDP-GlcA (blue). UDP-Api, UDP-Xyl and UDP-4-keto-pentose are shown in orange.

The specific activity of the GrUAXS S120C variant was 12.3 U/mg which is about 6-fold higher than the activity of GrUAXS wild-type. In a comparison, plant UAXS wild-type is about 7-fold more active than its C140S variant (Savino et al., 2019). Figure 36 shows the product distribution after 5 min and 30 min of reaction [see chapter 3.2.3; *(5)*].

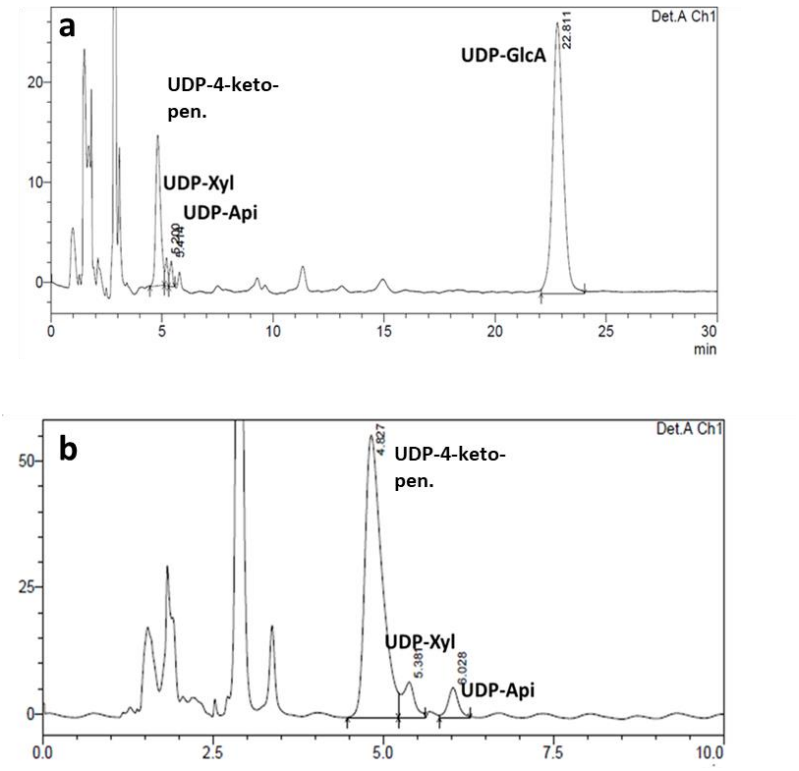

Figure 36. The HPLC chromatograms showing the products (UDP-Api, UDP-Xyl and UDP-4-keto-pentose) distribution and ratios of the GrUAXS S120C reaction with UDP-GlcA after 5 min (a) and after 30 min (b). UDP-4-keto-xyl : UDP-xyl : UDP-api = 10 : 1 : 1 is products ratio after 5 min (a). UDP-4-keto-xyl : UDP-xyl : UDP-api = 15 : 1.5 : 1 is product ratio after 30 min (b)

The enzyme produces UDP-4-keto-pentose in excess, but the result needs to be intepreted with a precaution considering that not a pure enzyme was used here and there was a possibility that the UDP-GlcA decarboxylase (ArnA) that was present in *E. coli* BL21 (DE3) LEMO21 also might accepted the substrate and converted it to UDP-4-keto-pentose (Borg et al., 2021a).

5. CONCLUSIONS

Based on results presented in this work following conclusions can be drawn:

1. UDP-GlcA methyl ester, a substrate analogue for human UDP-Xylose synthase (UXS), UDP-Apiose/Xylose synthase (UAXS) from *Arabidopsis thaliana* and UDP-glucuronic acid 4-epimerase (UGAepi) from *Bacillus cereus*, was successfully synthesized by the two step enzymatic route. Ethanol precipitation method for isolation of the produced UDP-GlcA methyl ester was optimized and resulted in about 96 % purity of the substrate analogue. The optimized precipitation method enables circumvention of traditional isolation methods, which have low efficiency, gave about 11.1 mg of UDP-glucuronic acid methyl ester. In this way specific substrate analogue was obtained and thus enabled investigation of the importance of specific amino acid residues in active site of UXS and UAXS and also UGAepi, which are responsible for decarboxylation or epimerization of the substrate, respectively.

2. Short-chain dehydrogenases/reductases epimerase (UGAepi) and decarboxylases (UXS and UAXS) were sucessfuly expressed in *E coli* strains and purified to homogeneity with high yield (the later two enzymes with yield of 34.8 mg/ml and 11.0 mg/ml, respectively, this thesis). Both decarboxylases, UXS and UAXS, accepted UDP-GlcA methyl ester as the substrate and showed activity towards this analogue (0.71 U/mg and 0.03 U/mg, respectively) that was comparable to the activity towards natural substrate – UDP-glucuronic acid (UDP-GlcA) of 1.6 U/mg and 0.15 U/mg, respectively. Further investigation is required to reweal more details of reaction mechanisms.

3. UGAepi activity towards its natural substrate UDP-GlcA (0.53 U/mg) was compared to the activity towards UDP-GlcA methyl ester (0.65 U/mg) and since UDP-GlcA methyl ester does not have a negatively charged carboxylate, UGAepi performs the faster epimerization of the substrate analogue than epimerization of UDP-GlcA.

4. Newly established enzymatic methanol assay supported the assumptions that (a) UXS and UAXS hydrolyze the ester bond in UDP-GlcA methyl ester before the decaborxylation reaction while (b) UGAepi does not hydrolyze the ester bond in the substrate analogue.

5. In addition, gene encoding UAXS from *Geminococcus roseus* (GrUAXS, an enzyme lacking cysteine residue in its active site), was successfully inserted in pET28a_GrUAXS plasmid and, after transformation of *E. coli* BL21 (DE3) LEMO21, expressed (5.7 mg of GrUAXS per liter of *E. coli* BL21 (DE3) LEMO21 cell culture). The heterologuous enzyme had lower activity towards UDP-GlcA than plant UAXS (an enzyme with the cysteine residue in its active site). In line with this finding, GrUAXS S120C variant was obtained (2.5 mg of GrUAXS S120C per liter of *E. coli* BL21 (DE3) LEMO21 cell culture) and showed significantly higher activity (12.3

mU/mg) than wild-type GrUAXS (2.1 mU/mg) supporting the importance of cysteine residue in the active site of the enzyme.

6. LITERATURE

Allard, S.T.M., Giraud, M.F., Naismith, J.H. (2001) Epimerases: Structure, function and mechanism. *Cell. Mol. Life Sci.* **58**, 1650-1665.

Borg, A.J.E., Beerens, K., Pfeiffer, M., Desmet, T., Nidetzky, B. (2021a) Stereo electronic control of reaction selectivity in short-chain dehydrogenases: Decarboxylation, epimerization, and dehydration. *Curr. Opin. Chem. Biol*. **61**, 43-52.

Borg, A.J.E., Dennig, A., Weber, H., Nidetzky, B. (2021b) Mechanistic characterization of UDP-glucuronic acid 4-epimerase. *FEBS J.* **288**, 1163–1178.

Cardenas, J.M. (1982) Pyruvate kinase from bovine muscle and liver. *Method. Enzymol.* **90**, 140–149.

Eixelsberger, T., Sykora, S., Egger, S., Brunsteiner, M., Kavanagh, K.L., Oppermann, U., Brecker, L., Nidetzky, B. (2012) Structure and mechanism of human UDP-xylose synthase: Evidence for a promoting role of sugar ring distortion in a three-step catalytic conversion of UDP-glucuronic acid. *J. Biol. Chem.* **287**, 31349–31358.

Harper, A.D., Bar-Peled, M. (2002) Biosynthesis of UDP-xylose. Cloning and characterization of a novel arabidopsis gene family, UXS, encoding soluble and putative membrane-bound UDP-glucuronic acid decarboxylase isoforms. *Plant Physiol.* **130**, 2188–2198.

Jörnvall, H., Krook, M., Persson, B., Atrian, S., Gonzàlez-Duarte, R., Jeffery, J., Ghosh, D. (1995) Short-Chain Dehydrogenases/Reductases (SDR). *Biochemistry-US* **34**, 6003–6013.

Kallberg, Y., Oppermann, U., Persson, B. (2010) Classification of the short-chain dehydrogenase/reductase superfamily using hidden Markov models. *FEBS J.* **277**, 2375–2386.

Kallberg, Y., Persson, B. (2006) Prediction of coenzyme specificity in dehydrogenases/reductases. A hidden Markov model-based method and its application on complete genomes. *FEBS J*. **273**, 1177-1184.

Kavanagh, K.L., Jörnvall, H., Persson, B., Oppermann, U. (2008) Medium- and short-chain dehydrogenase/reductase gene and protein families: The SDR superfamily: Functional and structural diversity within a family of metabolic and regulatory enzymes. *Cell. Mol. Life Sci*. **65**, 3895-3906.

Lemmerer, M., Schmölzer, K., Gutmann, A., Nidetzky, B. (2016) Downstream Processing of Nucleoside-Diphospho-Sugars from Sucrose Synthase Reaction Mixtures at Decreased Solvent Consumption. *Adv. Synth. Catal.* **358**, 3113–3122.

Maertens, B., Spriestersbach, A., Kubicek, J., Schäfer, F. (2015) Strep-Tagged Protein Purification. *Method. Enzymol*. **559**, 53–69.

Oppermann, U., Filling, C., Hult, M., Shafqat, N., Wu, X., Lindh, M., Shafqat, J., Nordling, E., Kallberg, Y., Persson, B., Jörnvall, H. (2003) Short-chain dehydrogenases/reductases (SDR): The 2002 update. *Chem-Biol. Interact*. **143**, 247–253.

Pieslinger, A.M., Hoepflinger, M.C., Tenhaken, R. (2010) Cloning of glucuronokinase from Arabidopsis thaliana, the last missing enzyme of the myo-inositol oxygenase pathway to nucleotide sugars. *J. Biol. Chem.* **285**, 2902–2910.

Rapp, C., van Overtveldt, S., Beerens, K., Weber, H., Desmet, T., Nidetzky, B. (2021) Expanding the Enzyme Repertoire for Sugar Nucleotide Epimerization: the CDP-Tyvelose 2-Epimerase from Thermodesulfatator atlanticus for Glucose/Mannose Interconversion. *Appl. Environ. Microb.* **87**, 1–14.

Savino, S., Borg, A.J.E., Dennig, A., Pfeiffer, M., de Giorgi, F., Weber, H., Dubey, K.D., Rovira, C., Mattevi, A., Nidetzky, B. (2019) Deciphering the enzymatic mechanism of sugar ring contraction in UDP-apiose biosynthesis. *Nat. Catal.* **2**, 1115–1123.

Smith, J.A., Bar-Peled, M. (2017) Synthesis of UDP-apiose in Bacteria: The marine phototroph Geminicoccus roseus and the plant pathogen Xanthomonas pisi. *PLOS ONE.* **12**, 1-21.

Spriestersbach, A., Kubicek, J., Schäfer, F., Block, H., Maertens, B. (2015) Purification of His-Tagged Proteins. *Method. Enzymol*. **559**, 1–15.

Vlnet, B. (1987). An Enzymic Assay for the Specific Determination of Methanol in Serum. *Clin. Chem*. **33**, 2204-2208.

Wang, W., Malcolm, B.A. (1999) Two-stage PCR protocol allowing introduction of multiple mutations, deletions and insertions using QuikChange(TM) Site-Directed Mutagenesis. *Biotechniques* **26**, 680–682.

Yin, Y., Huang, J., Gu, X., Bar-Peled, M., Xu, Y. (2011) Evolution of plant nucleotide-sugar interconversion enzymes. *PLOS ONE* **6**, 1-10.

STATEMENT OF ORIGINALITY

This is to certify, that the intellectual content of this thesis is the product of my own independent and original work and that all the sources used in preparing this thesis have been duly acknowledged.

Fran Debanić

Fran Debanić